Spring 2019

Archaeological investigation using geophysical methods to locate historic Byram's Ford Road

Marshall Seth Foster

Department:

ARCHAEOLOGICAL INVESTIGATION USING GEOPHYSICAL METHODS TO LOCATE HISTORIC BYRAM'S FORD ROAD

by

MARSHALL SETH FOSTER

A THESIS

Presented to the faculty of the Graduate School of the

MISSOURI UNIVERSITY OF SCIENCE AND TECHNOLOGY

In Partial Fulfillment of the Requirements for the Degree

MASTER OF SCIENCE

in

GEOLOGICAL ENGINEERING

2019

Approved by:

Neil L. Anderson, Advisor

J. David Rogers

Evgeniy V. Torgashov

ABSTRACT

Ground penetrating radar, a time domain electromagnetic metal detector and a frequency domain electromagnetic metal detector were used with the goal of locating a section of the Byram's Ford Road believed to be intersecting the historic Big Blue Battlefield in the Westport area of Kansas City, Missouri.

Ground penetrating data were acquired at three sites, Site A, Site B, and Site C. The time domain EM metal detector was used to acquire data at Site A, where subsequent ground truthing was conducted using the frequency domain EM metal detector and an excavation tool. Significant anomalies were visible on both the ground penetrating radar traverse profiles and the time domain EM profiles.

At Site A, most of the anomalies seen on the ground penetrating radar traverse profiles were attributed to a previously existing railroad. These anomalies appeared on each profile at the north end of Site A and appear as high amplitude reflections spanning approximately 10 feet across. Many localized anomalies appeared on the time domain EM data, which were then investigated in the ground truthing process. Only old farm equipment, including a fender, a wheel, and many wire pieces were found in this ground truthing process. The anomalies identified at Site C are likely caused by buried utilities, likely electrical lines used for the building bounding the west of Site C. The anomalies at Site B appear at the same distance along each traverse profile as high amplitude reflections. These anomalies are approximately 10 to 15 feet and are similar to those seen at Site A. These anomalies could be due to Byram's Ford Road, compacted soils caused by construction of the previously existing railroad, or an excavation.

ACKNOWLEDGEMENTS

I would like to thank Dr. Neil Anderson for providing this interesting thesis topic for me, and for his patient assistance in the technical editing of this paper. I would also like to thank Dr. Evgeniy Torgashov for his guidance in data acquisition and processing. I would also like to thank James Hayes and Marc Radloff for participating in data acquisition. Further, I would like to thank Dr. J. David Rogers for being on my committee and for his assistance and guidance during my graduate studies.

Past the wonderful faculty and peers that I have had the honor of working beside, I would like to express my appreciation for the support and encouragement I have received from my parents, Bryan and Cheri Foster, as well as my significant other, Jaimie Taylor.

TABLE OF CONTENTS

LIST OF ILLUSTRATIONS

Page

LIST OF TABLES

Page

1. INTRODUCTION

Geophysical data was acquired at Big Blue Battlefield in Kansas City, Missouri using ground penetrating radar (GPR), a time domain electromagnetic (TDEM) metal detector, and a frequency domain electromagnetic (FDEM) metal detector. These tools were chosen due to their previous applications in archaeological studies. The data was acquired with the purpose of locating a portion of historical Byram's Ford Road. Three sites, Site A, Site B, and Site C were identified as areas of interest for the project. Anomalies were identified at each of these sites. The anomalies at Site A were investigated further using the TDEM metal detector and the FDEM metal detector. The anomalies at sites B and C were attributed to buried utilities and past excavations.

1.1. BIG BLUE BATTLEFIELD & BYRMA'S FORD ROAD

Big Blue Battlefield is a historic Civil War battlefield located in Kansas City, Missouri. This battlefield is the location of one of the most important battles in Missouri during the Civil War. In order for both the Union and Confederate troops to reach this battlefield, they followed a path called Byram's Ford Road. Segments of Byram's Ford Road have been mapped in the Big Blue Battlefield Park as well as other segments being located to the west of the park. The locations that this project was conducted on are areas where the location of the path is unknown. Between the time that the battle took place and the present, this battlefield has been used for a variety of purposes. Currently, the battlefield site partially hosts an industrial park. A railroad intersects the battlefield site on the western edge, a portion of the railroad once cut from the west to the east through

the battlefield site, and many roads are laid to the north of the site. It is also reported that the battlefield site was used as farmland, likely for crops, subsequent to the Civil War.

1.2. ARCHAEOLOGICAL CASE STUDIES

Ground penetrating radar (GPR) may be employed in archaeological studies as it allows the user to map buried features that would otherwise not be seen when using traditional field methods. This imaging technique has been employed to locate historic Viking routes in Denmark (Sensors & Software), buried tombs, walls (Leucci and Negri, 2005), and many other objects of archaeological importance.

Time domain electromagnetic metal detectors have also been employed for archaeological studies. Most often, these metal detectors have been used in locating unexploded ordnance and munitions (McNeill and Bosnar, 2000).

1.2.1. GPR to Locate Historic Viking Routes in Denmark. Archaeologists in Denmark wished to locate historic Viking routes and identify building practices used in their roads. Before the investigation began, it was known that rocks and timber were used in road construction during this time. Further, it was known that the soil at the site was a soft peaty soil. This means that the road would likely have been pushed down and overlain by fresh soil and vegetation, thus no surface expression identifying the road can be seen.

Ground penetrating radar was employed to image this historic Viking route. The team used a 100 MHz antenna to compensate for the attenuation to be encountered in the soft peaty soil. The use of the lower frequency antenna allowed their investigation to image to a depth of approximately 10.5 feet. Their survey was successful as seen in

Figure 1.1 and Figure 1.2 which show the GPR data profile and an image overlay depicting the road construction. The overlain cross section on the GPR data profile appears to match the recorded high amplitude reflections, indicating that they had located the historic Viking route. This investigation was completed in less than five hours.

The rapid acquisition, real-time data analysis, and digital data recording for future processing and interpretation made the GPR method an adequate tool for this investigation.

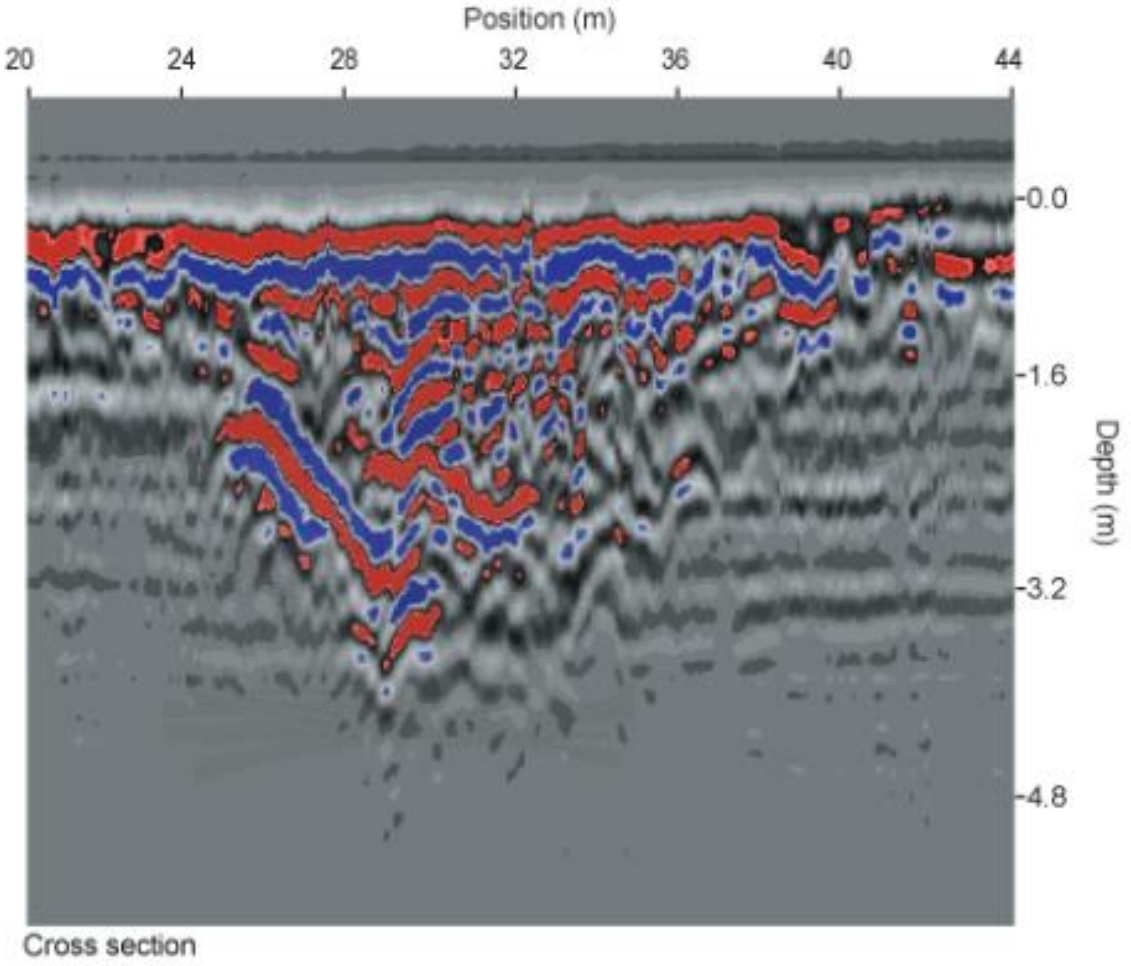

Figure 1.1: GPR profile of buried Viking route.

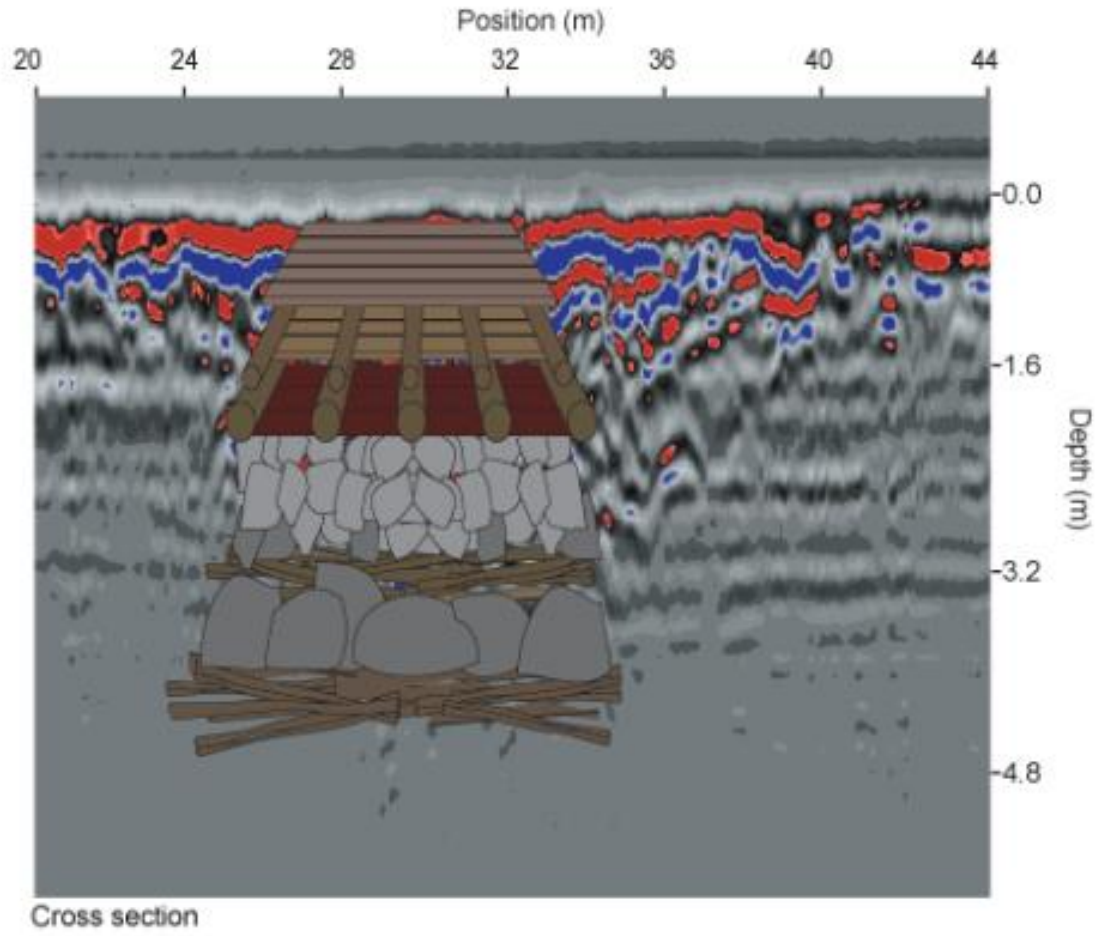

Figure 1.2: Road construction overlay on GPR profile.

1.2.2. GPR to Map Historic Living Features in Mesagne, Italy. Archaeologists in Italy wished to map archaeological features from the Messapian to Roman imperial age underneath an existing house, area A, and within proximity to previously discovered Messapian tombs, area B (Leucci and Negir, 2005). These tombs could either have been in the form of grave pit tombs or hypogeum tombs. It was also likely that these sites might contain remnants of a castle.

Two different antennas were used for the different survey objectives. A 200 MHz antenna and a 500 MHz antenna were used. For accurate interpretation, the data recorded inside the house had to be processed to remove reflections and diffractions from the

building materials. Once the data had been processed, both 2D and 3D maps were created for thorough understanding of reflection amplitudes.

This investigation yielded possible locations of hypogeum tombs at area A and possible road boundary walls at area B, as seen in Figure 1.3. The profiles depicting reflections from these archaeological features are shown below.

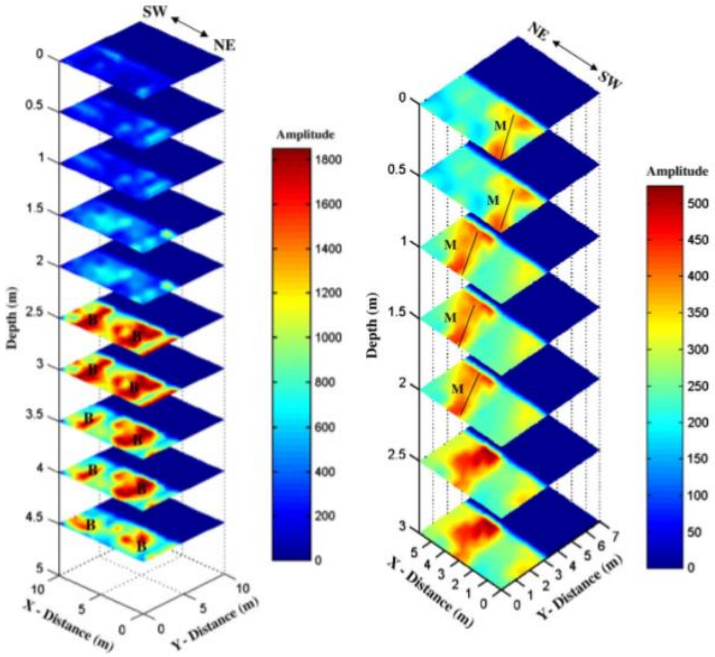

Figure 1.3: 2D time slices showing the potential hypogeum tombs (left) and potential boundary walls (right).

1.2.3. TDEM Metal Detector to Locate Various Buried Metallic Targets. In this case study, presented by Geonics Limited (McNeill and Bosnar, 2000), a variety of metallic targets were placed at the University of Waterloo “Columbia Test Site” to demonstrate the applications of their EM-63 TDEM metal detector.

Nine metallic targets of differing shapes, sizes, and metallic properties were placed on the site surface. These differences were selected to represent differences

between ferrous and non-ferrous materials, and the differences between spherical objects, scrap materials, and unexploded ordnance. In addition to these nine metallic targets placed on the surface, multiple drums and pipes of various sizes were buried at various depths.

This study showed the importance of using multiple time gates in a TDEM investigation. At the earliest time gate, each of the objects were clearly visible, while at a later time gate only two of these were visible. This study also demonstrates the differing time decay responses from different buried objects. In specific, a steel plate, Figure 1.4, and a steel drum, Figure 1.5, both buried at 1m depth show different responses. The steel drum time decay response demonstrates how the time decay response for a specific object only varies with depth, and not with shape.

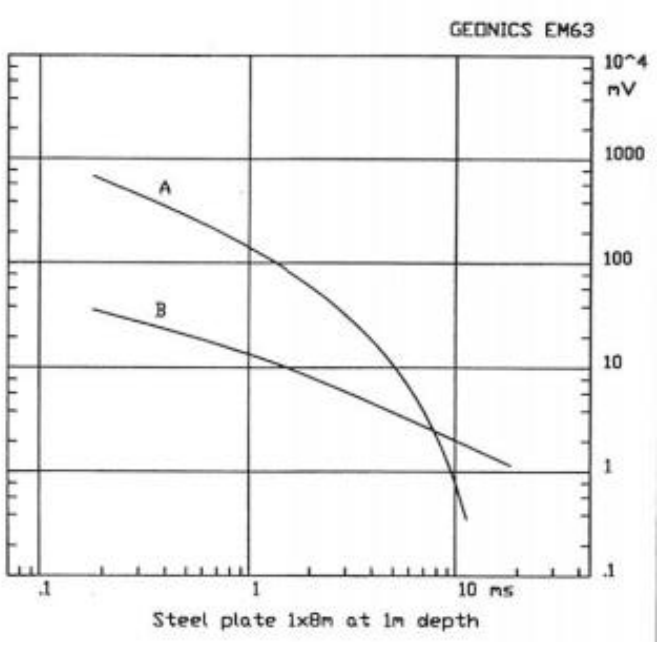

Figure 1.4: Steel plate time decay response curve A at center of plate, curve B at edge of plate.

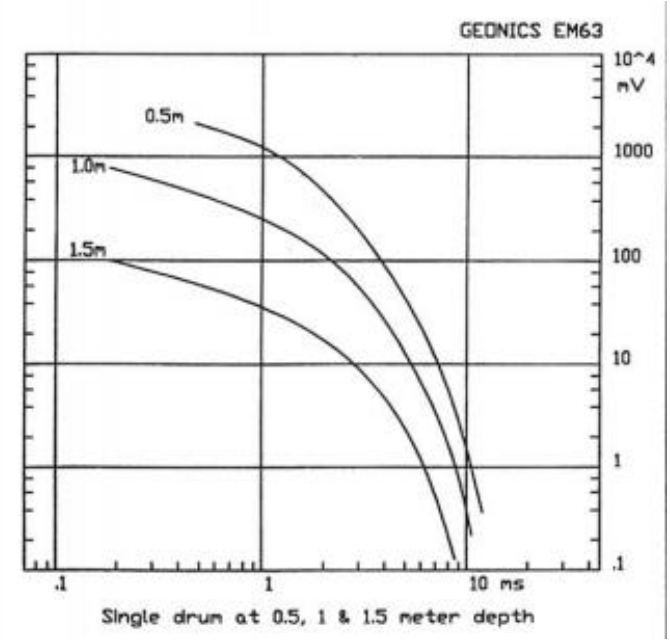

Figure 1.5: Steel drum time decay response at various depths.

1.3. INVESTIGATION OBJECTIVES

The purpose of this investigation was to accurately locate the historical Byram's Ford Road using ground penetrating radar and a time domain electromagnetics metal detector. In addition, multiple anomalies of interest were investigated using a frequency domain electromagnetic metal detector and excavated. This ground-truthing was conducted at the request of Daniel Smith, Chairman of the Board of the Monnett Battle of Westport Fund for the Civil War Round Table of Kansas City, in the hopes of acquiring artifacts from the Civil War.

2. SITE HISTORY

2.1. MISSOURI'S INFLUENCE IN THE CIVIL WAR

Missouri held a powerful position for whoever could claim it, the Union or the Confederates, in the Civil War. At the start of the war, Missouri had only recently began expanding its railroad systems throughout the state with lines converging on St. Louis. This provided access to the abundant mineral recourses in the southern part of the state as well as the agricultural resources in the north. St. Louis was also an important city because it was situated at the confluence of the Missouri River and Mississippi River.

Control of St. Louis meant control of the Missouri River and the Mississippi River. Control of these two rivers also granted influence over the Ohio River, which joins the Mississippi River further south in Illinois. Also, at St. Louis was the federal arsenal, an institution that housed enough equipment to arm an entire army. In order to establish reliable control of this critical city, control of the entire state was needed. (shsmo.org)

2.2. THE BATTLE OF WESTPORT

General Sterling Price, a man who sought conquering the powerful state of Missouri for the confederates, set on one of the largest cavalry raids of the American Civil War in September of 1864. His raid began at Pilot Knob, where his troops were significantly diminished. They then moved north to the Missouri River. To avoid defeat by Union forces from St. Louis, the Confederates headed west to Kansas City. Part of his military objective was to help confederate refugees and to protect and transport large amounts of weapons and other resources vital to his campaign.

In order to do so, the Confederates used a massive wagon train comprised of 600 wagons, each likely being approximately 4 feet from wheel to wheel (Antique Ordinance) and 3,000 cattle (Smith). This massive wagon train made its way through Missouri by use of the Santa Fe Trail and its counterpart, Byram's Ford Road. By October 19, Price was moving through Lexington and on October 22 his cavalry encountered Union troops blocking Byram's Ford Road at the site of the Battle of Big Blue, Big Blue Battlefield. The following day, Price and his men were defeated at the Battle of Westport, forcing the Confederates out of the state ("Price's Missouri Expedition").

The location known as Big Blue Battlefield consists of a heavily wooded region and a slightly dipping meadow separated by the Big Blue River. The wooded region lies to the east of the river, and the meadow lies to the west of the river. The meadow is bounded on the east side by the river and on the west side by a limestone bluff.

When the Confederates were moving west, they emerged from the wooded region and crossed the river into the meadow following Byram's Ford Road. Union forces were encountered on the west bank of the Big Blue River and were defeated. This granted the Confederates control of the meadow and the limestone bluff.

Union troops lead by General Alfred Pleasonton followed Byram's Ford Road behind the Confederate forces (thecivilwarmuse.com). When these Union troops reached the Confederates, the meadow was already under Confederate control, and another battle began. Once this battle began, the Confederates were forced up onto the bluff, giving them the advantage. The Union troops were then in a position where pushing forward resulted in casualties and retreating resulted in casualties (battlefields.org). This meadow is now referred to as the Big Blue Battlefield, the Battle at Byram's Ford, and Byram's

Ford Road. A map of this battle taken from Howard N. Monnett's "Action Before Westport" is displayed in Figure 2.1.

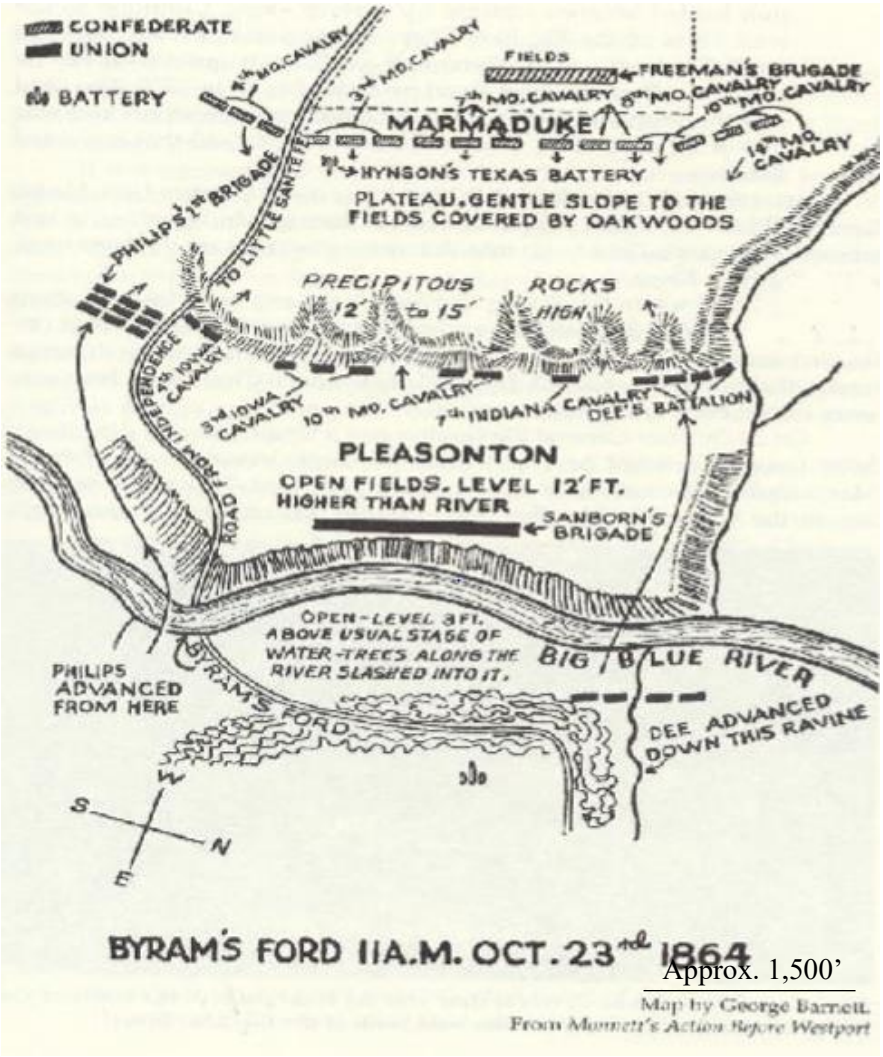

Figure 2.1: Map displaying military positions of both Union and Confederate forces.

The numerous casualties at Byram's Ford Road led to the eventual retreat of Price's forces granting the Battle at Byram's Ford, Big Blue Battlefield, a Class B ranking by the Civil War Battlefield Sites Advisory Commission. This Commission was appointed by Congress and Secretary of the Interior to classify Civil War sites according to their historical significance and importance and well as define their conditions and to

recommend preservation tactics. The rankings were from A to D; A meant the battle had a decisive impact on the campaign and thus the war, B was assigned to battles that only had an impact on the campaign, C rankings were given to battles that had an influence of the campaign, and D only affected local objectives and not the campaign directly (nps.gov, 1993). The high ranking given to Big Blue Battlefield and the importance of Byram's Ford Road in the battle itself holds high significance to historical societies in locating the old road.

2.3. PREVIOUS INVESTIGATIONS TO LOCATE BYRAM'S FORD ROAD

Multiple investigations have been conducted in attempt to both map the location of the historic Byram's Ford Road and to find Civil War artifacts. Just east of the study area (Figure 2.2), TRC Mariah Associates, Inc. (Marmor, 1997) performed an archaeological study with the purpose of locating and identifying Civil War related artifacts and any segments of Byram's Ford Road for the U.S. Army Corps of Engineers. The main purpose of their study was to indicate whether the site could undergo further development, or if development should be halted due to historical significance. During their study, they located three munition artifacts as well as multiple other artifacts associated with the war. However, they were not able to identify the location of Byram's Ford Road. They speculate that this could be a product of their investigation methods or simply due to the amount of disturbances civilization has caused the area over time (Marmor, 1997).

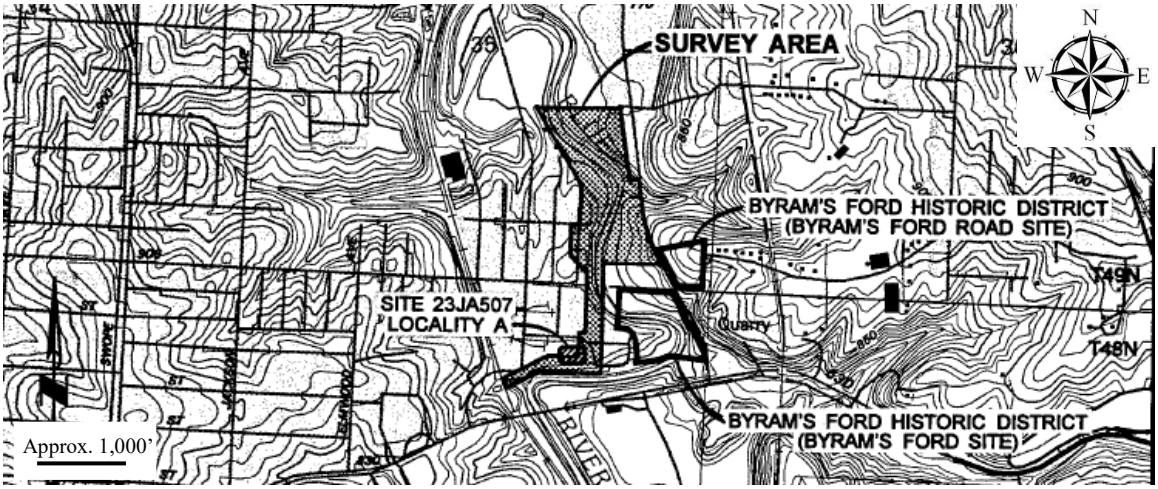

Figure 2.2: TRC Mariah Associates archaeological investigation survey area.

Three other surveys have been conducted in the vicinity of the study area that have either misidentified the location of the road or not attributed their findings to the presence of the road. These surveys were conducted by Commonwealth Associates, Inc. (Fitting et al, 1978), David R. Evans and David J. Ives (Evans and Ives 1980:14-15), and Jeffrey K. Yelton (Yelton 1993), respectively. The two investigations that misplaced the location of Byram's Ford Road placed the road at the 63rd Street Bridge. The third investigation did not report any Civil War artifacts or the location of Byram's Ford Road but was conducted at the same location as the previous two (Marmor, 1997).

Another investigation was conducted by Gray & Pape, Inc. (Miller and Walsh 1995), with the purpose of creating a preservation plan for the battlefield. This investigation took place to the west, south, and east of the study area and covered an extensive 240 acres. The investigation yielded possible field fortifications in three locations as well as three segments of Byram's Ford Road (Figure 2.3). These segments are on either side of the project area. Two of these segments lie to the east of the project area. The furthest segment cuts across the eastern bluffs leading down to the Big Blue

River. The closest one emerges from the river along the western terrace and cuts down an adjacent ravine. The third segment lies to the west of the project area and is almost entirely intact. This segment runs relatively west-east and is located atop the bluff containing the Pepsi-Cola building to the west of the project area. The placements and trajectories of these located segments of Byram's Ford Road seem to indicate that the road would be found in the study area.

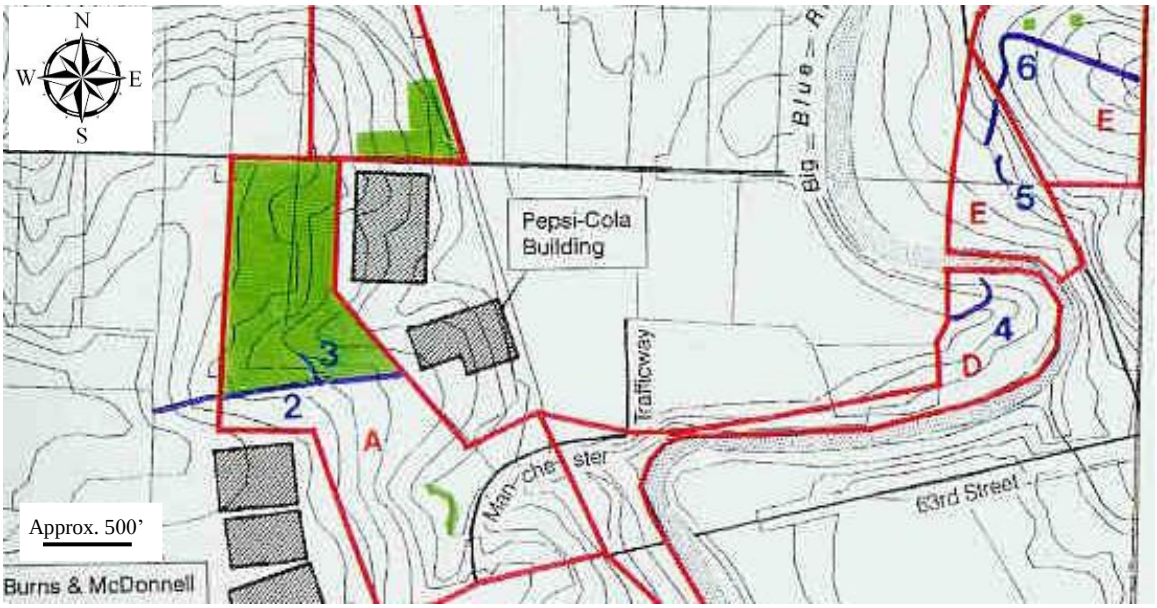

Figure 2.3: Gray & Pape archaeological investigation survey area(s).

Further, in a site development plan proposed by the Monnett Battle of Westport Fund, Inc., the exact known locations of Byram's Ford road are thoroughly discussed. Figure 2.4 shows a proposal for a trail to be constructed along the path of the known locations of Byram's Ford Road. The red line in this figure is a direct line from the ends of the known segments of Byram's Ford Road.

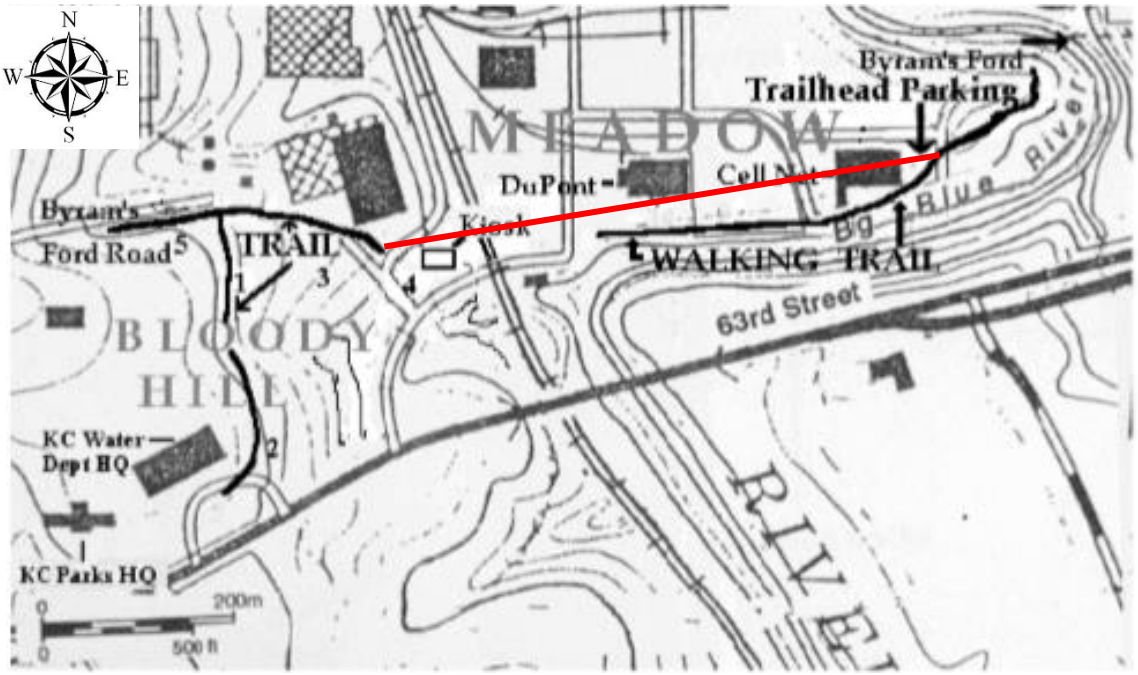

Figure 2.4: Site development plan for a walking trail.

In a search for historical maps of the project area, an atlas of Kansas City, Missouri was discovered. This atlas is from 1925. It appears that when this atlas was created, Byram's Ford Road was still intact, or at least visible. Figure 2.5 shows the image taken from the northwest quarter of Section 9, Township 48, Range 33. In Figure 2.5, Byram's Ford Road is clearly mapped, tracing to the north of a west to east facing segment of the Big Blue River. The archaeological investigation conducted by TRC Mariah Associates surveyed this area and did not find any segments of Byram's Ford Road. A majority of the existing roads had not been constructed at the time that this atlas was created. This makes identifying the current study area location difficult on this image, as the only reference markers are the railroad and the meanders of the river. More on the current study area location will discussed in a later section.

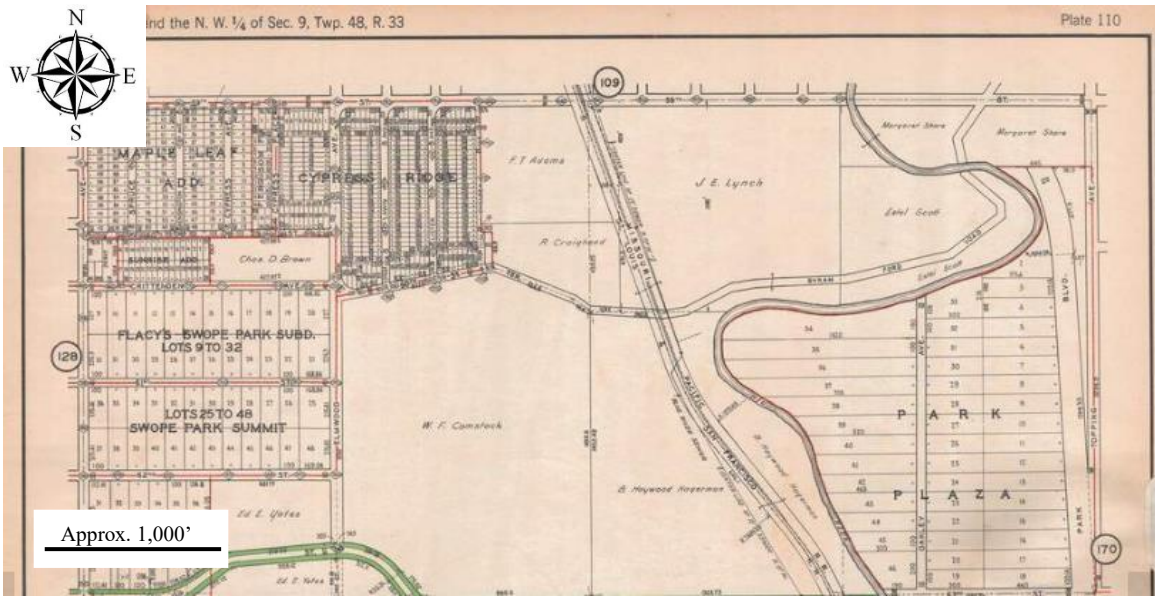

Figure 2.5: 1925 Kansas City Atlas image.

2.4. ENVIRONMENTAL SETTING

The study area is located in Kansas City, Missouri (Figure 2.6) and is just west of a prominent meander of the Big Blue River in southern Kansas City, MO. The Big Blue River, sometimes referred to as simply the Blue River, is a tributary of the Missouri River, and generally flows northward. Due to the meandering of its channel, it can be subject to lateral migration. The image below, Figure 2.4, shows a Google Earth image with a marker for the center of Site A, the largest portion of the study area, at an elevation of 778 ft above mean sea level, a marker for a meander of the channel at an elevation of 746 ft above mean sea level, and a marker for a Bethany Falls outcrop at 789 ft above mean sea level. The two red arrows on the image indicate the location of two concrete slabs, one significantly larger the other.

The site is covered with what has been classified by the Natural Resources Conservation Service of the United States Department of Agriculture as a udarents-urban

land complex. This soil is composed of silt loam for the upper 5 inches, with silty clay loam underlying to a depth of approximately 80 inches with a percent clay of approximately 27%, where the water table and bedrock can then be found. This soil classification is likely due to the use of this land as farmland in the past, granting the shallow subsurface with less clayey materials. The urbanization of this land over the past 50 years has likely been another contributing factor to the soil type at this location. The location of this project site in relation to the Big Blue River also has had a large impact on the soil type, as if flooding has occurred in the past, clayey and silty sediments will be deposited in the project area. The bedrock in this area is composed of Pennsylvanian age limestones, sandstones, and shales (USGS, 2018). To the west of the study area, marked on Figure 2.7 by the Bethany Falls marker, shows an outcrop of limestone that marks an edge of the Big Blue River floodplain. This specific outcrop is believed to be one of the obstacles encountered by Union forces on the second day of the Battle of Big Blue.

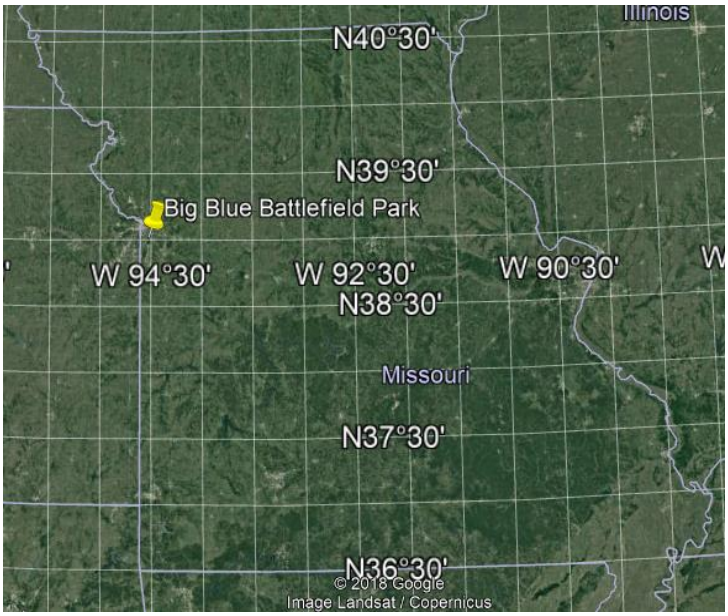

Figure 2.6: The location of Big Blue Battlefield Park.

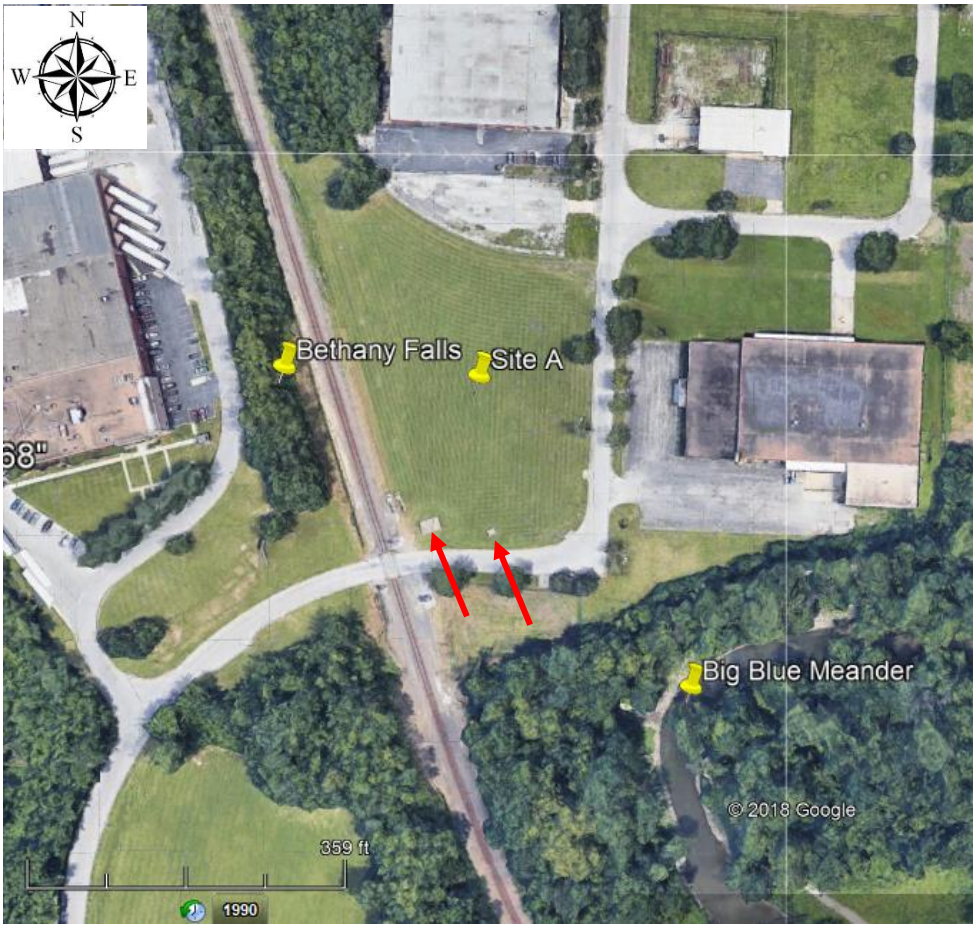

Figure 2.7: Google Earth image of the project location with Site A marked with respect to Big Blue River and Bethany Falls limestone.

3. GROUND PENETRATING RADAR (GPR)

3.1. BASIC THEORY

The basic GPR set up consists of a control unit and a dual transmitter/receiver antenna. The antennas range in frequencies in the electromagnetic (EM) wavelengths and are used to generate EM pulses. These EM pulses propagate through the subsurface at a velocity equal to a function of the material's dielectric permittivity. When an EM pulse encounters an interface of varying dielectric permittivity in the subsurface, some of the energy is reflected, scattered, or transmitted by that interface. A portion of the reflected energy, as well as noise, will be recorded by the receiving antenna. All recorded energy carries with it information about the two way travel time, or simply the travel time, and amplitude. From these we can determine apparent depth based on the selected dielectric permittivity.

3.1.1. Propagation Velocity. Electromagnetic wave propagation velocity through a material is the defining principal of the GPR technique. Propagation velocities are highly dependent on the electrical and magnetic properties of the material the EM waves are passing through. The equation used to calculate this velocity is $v=C/\varepsilon^{1/2}$, where v is the propagation velocity, C is the speed of light, and ε is the dielectric permittivity of the material. Since air has a dielectric permittivity approximately equal to 1, the velocity of an EM wave propagating through air is equal to C. All earthen material has a dielectric permittivity greater than air, meaning that the propagation velocity through earthen material will always be less than C (Daniels, 2000). This also means that the travel time through earthen material will always be greater than the same distance traveled through

air. A simplified diagram showing a vertically incident path from a GPR unit is shown below (Figure 3.1).

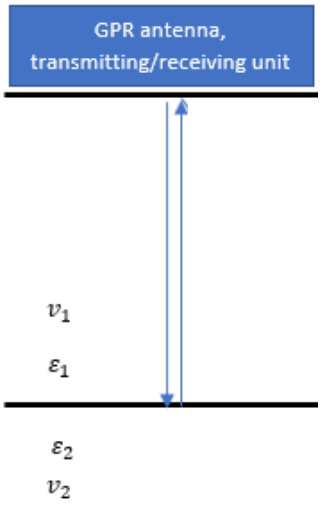

Figure 3.1: Schematic showing two-way travel time for a vertically incident travel path.

3.1.2. Dielectric Permittivity. By the equation for propagation velocity, the dielectric permittivity of a material directly determines the velocity of the EM pulse propagating through that material. The dielectric permittivity is a parameter related to the water content, magnetic, and electric properties of the material. In a basic sense, dielectric materials store energy when exposed to an electric field. Energy storage is generated by the atoms reorienting themselves to balance their charges with the new external charges. This movement results in energy loss and is related to attenuation by the loss tangent, which will be discussed later (Part 3.1.3). Table 3.1 shows expected dielectric permittivity values and their corresponding velocities. By looking at the first two rows, air and water, the effect of the presence of water can easily be seen. This

relationship is further demonstrated by the rest of the materials listed with their dry and wet dielectric permittivity's listed. Understanding the dielectric permittivity relationships in different materials is crucial for selecting the correct antenna frequency to be used at the site.

Table 3.1: Dielectric permittivity's of some geologic material and their respective velocities (adapted from: Baker, Jordan, and Talley, 2007)

Material	Dielectric Permittivity (ε)	Velocity (C) (m/ns)
Air	1	0.3
Fresh Water	81	0.03
Dry Sand	4-6	0.12-0.17
Wet Sand	10-30	0.05-0.09
Dry Sandstone	2-3	0.17-.021
Wet Sandstone	5-10	0.09-0.13
Dry Clay	2-6	0.12-0.21
Wet Clay	15-40	0.05-0.08
Loamy, Dry Soil	4-6	0.05-0.08
Loamy, Wet Soil	15-30	0.07-0.09

3.1.3. Attenuation or Loss. With the GPR method, attenuation, or energy loss, is caused by multiple factors. Assuming proper operation and antenna selection, four of these factors can be assumed to be negligible. These include antenna loss (antenna efficiency), antenna mismatch loss (how well antenna and transmitter are matched), transmission coupling loss (loss between antenna and material due to air), and

retransmission coupling loss (loss on return journey through the air). There remain three important factors to consider, spreading loss, scatter loss, and material attenuation loss.

As the EM wave propagates through the subsurface, it expands in three dimensions (Figure 3.2). Since the amount of energy available does not change, this results in a decrease in energy per unit area as both time and distance traveled increase and is referred to as spreading loss.

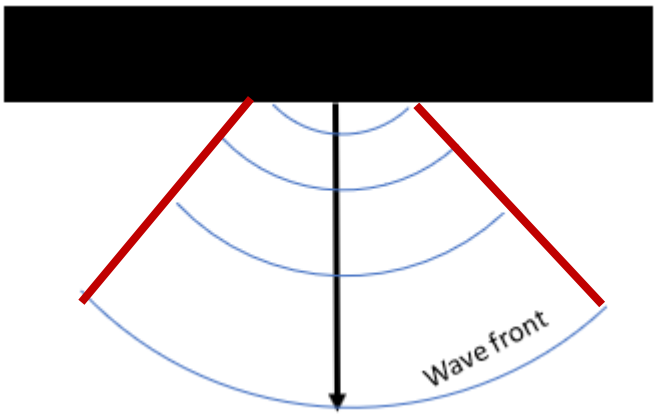

Figure 3.2: Propagating EM pulse through a medium. Blue lines show spreading loss.

When a wave front encounters an interface, some of the energy will be reflected to the receiver and some of the energy will be refracted through the material. Energy may also be diffracted from certain interfaces resulting in anomalous signals in data (Figure 3.3). These forms of energy transfer result in energy loss and is known as scatter loss which can be slightly limited by shielding the original pulse (Daniels, 2000). This results in a “flashlight effect,” where the energy travels in one direction like a flashlight. The red lines in Figure 3.2 represent this “shield.” Shielding the energy also removes issues related to EM radiation from surface sources.

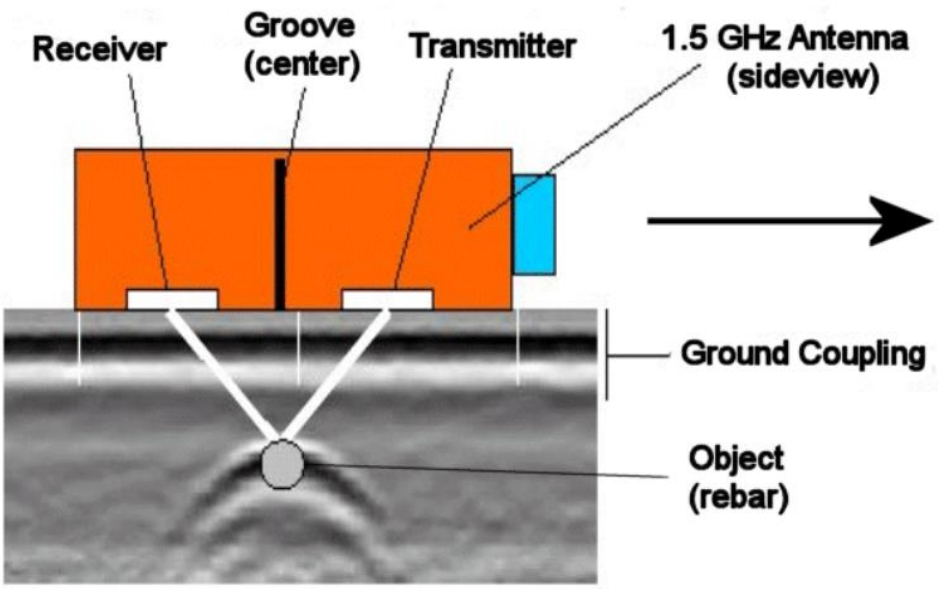

Figure 3.3: Schematic showing recorded diffractions from a piece of rebar.

When atoms reorient themselves to balance an external electrical field, some energy is lost, and some is stored, this ratio is known as the loss tangent or dissipation factor (Baker, Jordan, and Talley, 2007). The dissipation factor, along with frequency, dielectric permittivity, and magnetic susceptibly of the material and free space are all related to the material attenuation loss (Daniels, 2004). Attenuation of common materials encountered in the field are shown in Table 3.2 and a comparison of attenuation and dielectric permittivity's are shown in Table 3.3.

The high attenuation due to wet clay poses an issue for acquiring ground penetrating radar data in areas where clay is present. The attenuation will cause the actual depths imaged to be dramatically less than the desired depth.

Table 3.2: Common materials and loss at specified frequencies of 100 MHz and 1 GHz (Daniels, 2004)

Material	Loss at 100 MHz	Loss at 1 GHz
Clay (moist)	5–300 dB m^{-1}	50–3000 dB m^{-1}
Loamy soil (moist)	1–60 dB m^{-1}	10–600 dB m^{-1}
Sand (dry)	0.01–2 dB m^{-1}	0.1–20 dB m^{-1}
Ice	0.1–5 dB m^{-1}	1–50 dB m^{-1}
Fresh water	0.1 dB m^{-1}	1 dB m^{-1}
Sea water	100 dB m^{-1}	1000 dB m^{-1}
Concrete (dry)	0.5–2.5 dB m^{-1}	5–25 dB m^{-1}
Brick	0.3–2.0 dB m^{-1}	3–20 dB m^{-1}

Table 3.3: Dielectric permittivity of various geologic materials and their respective attenuation (adapted from: Daniels, 2004)

Material	**Dielectric Permittivity (ε)**	**Attenuation, dB/m**
Air	1	0
Fresh Water	81	0.01
Dry Sand	4-6	0.01-1
Wet Sand	10-30	0.5-5
Dry Sandstone	2-3	2-10
Wet Sandstone	5-10	4-20
Dry Clay	2-6	10-50
Wet Clay	15-40	20-100
Loamy, Dry Soil	4-6	0.5-3
Loamy, Wet Soil	15-30	1-6

3.1.4. Depth of Investigation and Resolution. It is important to note that the depth of investigation and both the spatial and vertical resolution are related to both the frequency of the antenna selected and the permittivity of the subsurface material. This means that proper antenna frequency selection is necessary for adequate data acquisition. In general, it holds that higher frequency antennas-from 500 MHz to 1GHz (Daniels, 2004) are optimal for resolutions less than 20 cm. Lower frequency antennas will have lower spatial resolution while having greater depths of penetration, and higher frequency antennas will have higher spatial resolution while having lesser depths of penetration. This relationship is presented in Table 3.4. However, in situations where the ground material has high attenuation properties, even the low frequency antennas will have very shallow depths of investigation. This is particularly apparent when wet clay is present and can cause issues with GPR acquisition in Missouri.

Table 3.4: The first and second choice antennas to use for certain depth ranges.

Depth Range of Interest	**Best Antenna**	**Second Best Antenna**
0-0.5m (0-1.5ft)	1600-2500MHz	900MHz
0-1m (0-3ft)	900MHz	400MHz
0-2.5m (0-8ft)	400MHz	270MHz
0-9m (0-30ft)	200-270MHz	100MHz
0-20m (0-60ft)	15-80MHz	100MHz
0->20m (0->60ft)	15-80MHz	100MHz

3.2. DATA ACQUISITION

Ground penetrating radar data was acquired at the Byram's Ford Road site in Kansas City, Missouri. This data was acquired using a 400 MHz antenna at three sites within the Byram's Ford Road site and will be referred to as Site A (Figure 3.4a), Site B (Figure 3.4b), and Site C (Figure 3.4c).

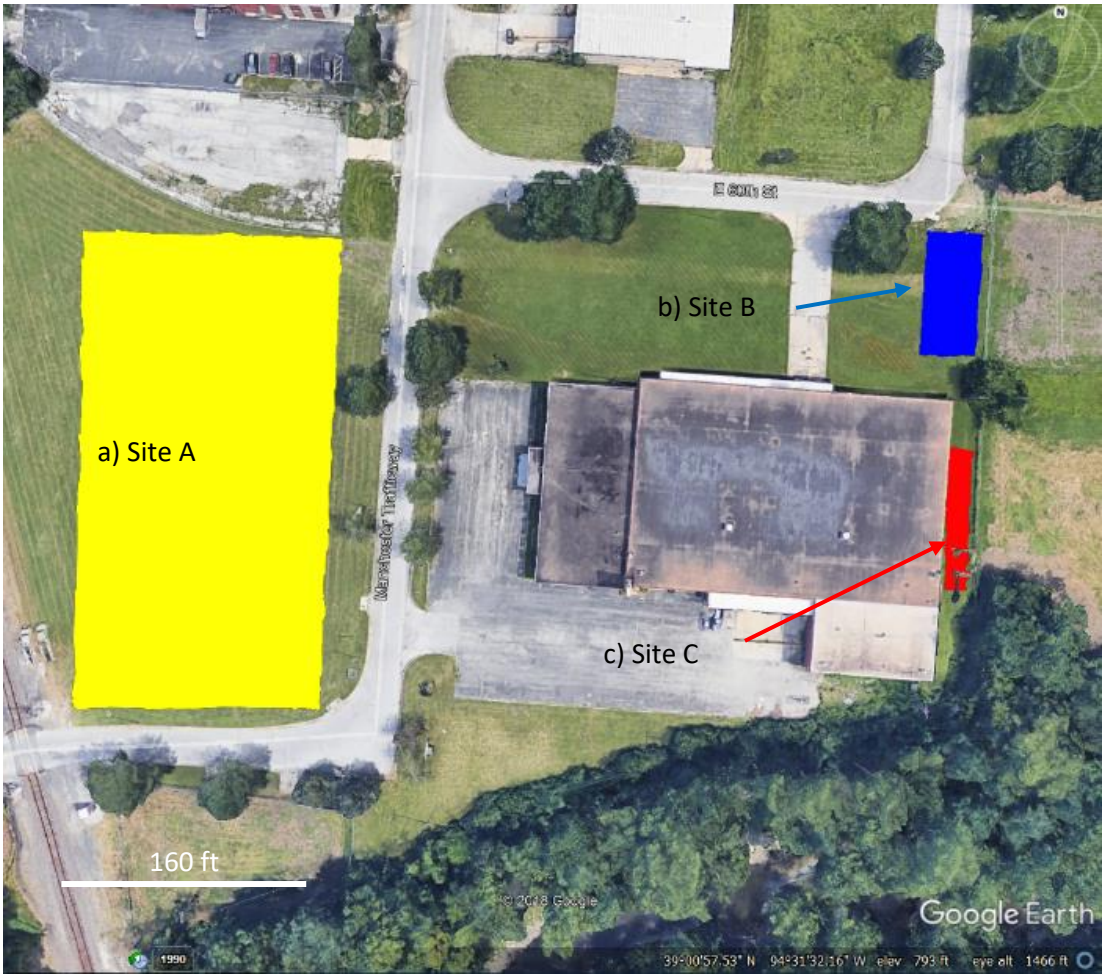

Figure 3.4: Big Blue Battlefield site with a) the Site A, b) Site B, and c) Site C.

At Site A, data were acquired at 10-foot intervals along a total of 53 profiles. Of these, 36 were oriented west-east and are hereby referred to as traverses 1-36, and 17 were oriented south-north and will be referred to as traverses 37-53 (Figure 3.5).

Photographs taken from the northeast corner of the site facing southwest and west are displayed in Figures 3.6 and 3.7, respectfully. On Figure 3.6 orange marker flags can be observed. These marker flags were used to indicate the east boundary of Site A and were spaced at 10 foot intervals. On Figure 3.7, more orange marker flags can be observed. These marker flags were used to indicate the north boundary of Site A and were also spaced at 10 foot intervals.

Upon arrival, only Site A was marked with orange marker flags to denote the desired traverses. These flags were small but were metal and slightly interfered with data acquired directly adjacent to them. Due to these marker flags, the original traverse 37 was used as a "test" and removed from the processing steps and was not included in interpretation.

Due to the first large slab in the southwest corner of the site, traverses 2 and 3 were started 27 feet east of the rest of the traverses oriented west-east. Traverse 2 was also split into two traverses at 69.4 feet by a 15-foot gap due to the second, smaller concrete slab, which can be seen in Figure 3.12. Traverses 50-53 began approximately 20 feet north of the starting points of the other traverses oriented south-north due to the large slab, and traverse 43 began 12 feet north due to the smaller slab. These reductions in traverse length had no significant effect on the data acquisition process.

At Site B, four parallel traverses oriented north-south were acquired, and at Site C, two parallel traverses oriented north-south were acquired (Figure 3.8). A photograph of Site B taken from the northwest corner facing southeast is displayed in Figure 3.9. A photograph of Site C taken from the north and facing south is displayed in Figure 3.10.

Figure 3.5: Site A GPR traverses.

Figure 3.6: Photograph facing southwest from the northeast corner of Site A.

Figure 3.7: Photograph facing west from the northeast corner of Site A.

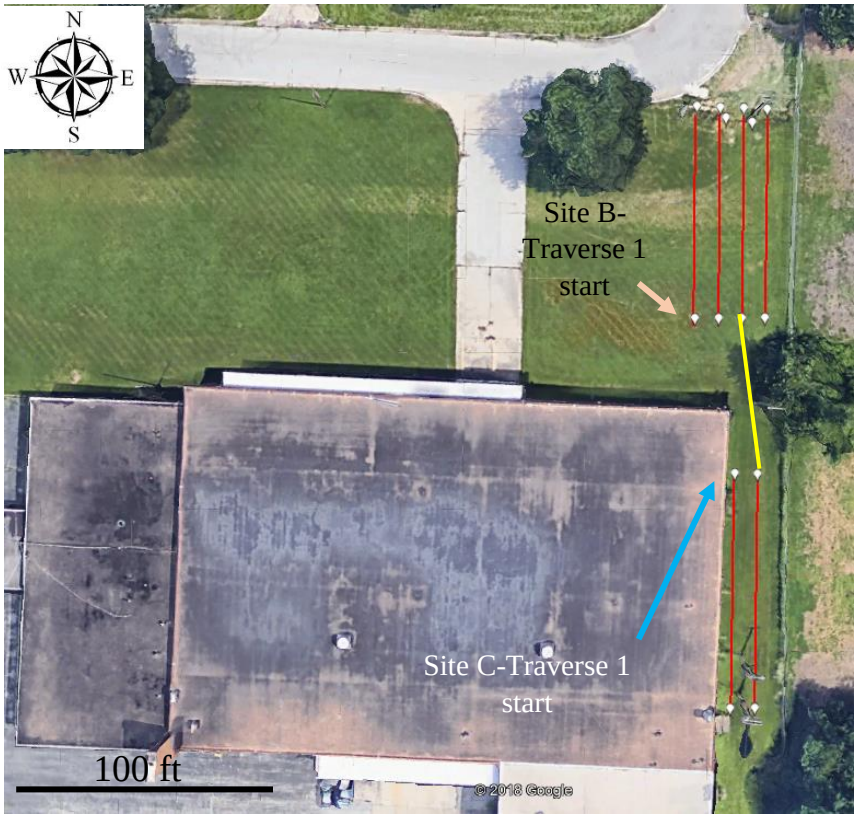

Figure 3.8: Orientation of Site B and Site C traverses.

Figure 3.9: Photograph facing southeast taken from the northwest corner of Site B.

Figure 3.10: Photograph facing south taken from the north end of Site C.

3.2.1. GPR Set Up. This investigation employed the SIR Systems-3000 manufactured by Geophysical Survey Systems, Inc (GSSI) to acquire GPR data. Upon arriving to the site, the survey cart first needed to be assembled. After this, the 400 MHz antenna was mounted and attached to the cart, as well as connected to the survey wheel. The SIR-3000 control unit was then set upon the survey cart and connected to the 400 MHz antenna (Figure 3.11). A 400 MHz antenna was selected with the hopes that it would allow for the greatest depth of penetration in the loamy soil with the highest resolution. The survey wheel is used for calibration and to allow for specified acquisition parameters.

Figure 3.11: Survey cart with antenna, control unit, and survey wheel.

As shown above (Tables 3.2 and 3.3), the dielectric permittivity of loamy/clayey soils range drastically depending on moisture content. On the day of acquisition, the top soil was moderately dry, though it had rained a small amount in the days prior. This, combined with the assumption that clay would be encountered at a depth of 5 inches, lead to the selection of a dielectric permittivity constant of 10 that represented an average between the values expected for wet and dry loamy soil and clay. The expected depth to the buried Byram's Ford Road would likely be between 6 inches and 2 feet. Using the 400 MHz antenna and the selected dielectric constant, the maximum depth expected to be reliably imaged to was around three feet, which is more than enough to image the target. However, since there is clay at the project area, and it had rained, any signal imaged at three feet would not be reliable.

A buried road will likely only be seen in a GPR profile as a horizontal zone of slightly higher amplitudes than the surrounding medium. This is a characteristic response

of more highly consolidated material when exposed to EM pulses. In order to more clearly see this, and to rule out any buried utilities, 48 scans per foot were used with 512 samples per scan. The sample range was limited to 30 nanoseconds, just slightly above the recommended minimum for a 400 MHz antenna (Table 3.5).

Table 3.5: Different frequency antennas and their applications (GSSI SIR-3000 User's Manual, 2009)

Frequency	Sample Applications	Typical Max Depth Feet (meters)	Typical Range (ns)
2.6 GHz	Structural Concrete, Roadways, Bridge Decks	1 (0.3)	10
1.6 GHz	Structural Concrete, Roadways, Bridge Decks	1.5 (0.5)	10-15
900 MHz	Concrete, Shallow Soils, Archaeology	3 (1)	10-20
400 MHz	Shallow Geology, Utility, Environmental, Archaeology	9 (3)	20-100
200 MHz	Geology, Environmental	25 (8)	70-300
100 MHz	Geology, Environmental	60 (20)	300-500

3.2.2. Data Acquisition. Acquisition began immediately after the GPR unit was set up. In order to assure correct navigation along correct traverses, tape measures were used. With a team of four, three began stretching out the tape measure for the next traverse, while the other acquired data (Figure 3.12). This process allowed for quick, efficient acquisition along straight, parallel traverses. Once the data for one traverse were collected, the unit was moved to the start of the next traverse. Each traverse was spaced 10 feet from the previous traverse.

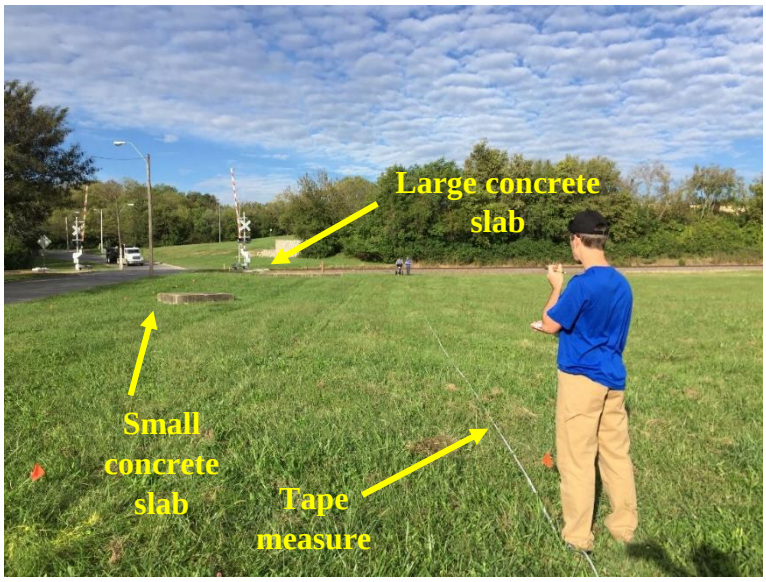

Figure 3.12: Photograph taken from the east side of Site A facing west. A tape measure is stretched out along a traverse to be acquired.

As GPR data is acquired, the control unit displays the data in real time, allowing for rapid, in field interpretation. Along the first few traverses, notes were taken of each anomaly as they were seen in real time. However, as the day went on and the sun moved overhead, it became increasingly difficult to see the screen's display, even with the sunshade attached. It was decided to only make notes of extreme anomalies and to carry on with acquiring the data, with the idea that any additional anomalies would be identified during data interpretation.

At Site A, data was first acquired along the west-east traverses. Due to the size of this site, each consecutive traverse was acquired in opposing directions. The first traverse was acquired from west-east and traced the southern boundary of Site A, the second traverse was set at 10 ft north of the first traverse and was acquired from east-west, and so forth, until all 36 traverses were acquired. Next, the north-south traverses were collected with the same principal, beginning with traverse 37. The first traverse acquired

was oriented north-south and was used as a test run. The second north-south traverse, but first to be used and thus is traverse 37, was oriented south-north and began at the south east corner of the site, followed by a north-south oriented traverse spaced at 10 feet to the west of the end of the second traverse.

Upon completing the GPR acquisition for Site A, acquisition at Site B and Site C began. At Site B, data was acquired along four traverses oriented north-south with 10 feet spacing. Each of these traverses were 60 feet long. The building and fence bounding Site C only allowed for two traverses to be acquired, both from north-south with a spacing of 10 feet between the two. An extra traverse, presented as the yellow line on Figure 3.8, was acquired between the start of the second traverse at Site C to the end of the second traverse of Site B.

3.3. DATA PROCESSING

The software used to process GPR data in this project is RADAN 7. Processing steps using this software is relatively straight forward in most cases. Data processing using RADAN is performed with the purpose of allowing all users to be able to process large data sets with ease (GSSI, 2007). This software has a multitude of processing steps available, but in most cases only a select few are needed.

3.3.1. Purpose of Processing GPR Data. As explained throughout Section 3.1, there are many issues involved with the propagation of GPR pulses through the subsurface. This may pose some issues when analyzing and interpreting the resulting data. Processing steps are then employed to minimize these issues. As mentioned, there

are many options for processing. However, only a handful of these steps are typically used, and in this specific project, very few are needed to accurately interpret the data.

3.3.2. Data Processing Steps. Data was acquired at Site A in alternating directions and were recorded in feet. To insure that the data is viewed using feet as the scale, the Vertical Units and Horizontal Units options are set as feet on the Home tab of RADAN 7. Since the first traverse was acquired from west to east, the second from east to west, and so on, the orientations of each file must be switched to where they all match. To do this, each even numbered file, all oriented east to west, were reversed and saved as a new file. Doing this set each of these files to be oriented west to east. These steps were also performed for the second set of data from Site A, where the first traverse was acquired south to north, the second north to south and so on. These files were all set to be oriented south to north. Once all of the files are oriented in the same direction, the user can open a batch of files containing all the files oriented in that direction. This allows for quicker and simpler processing.

During acquisition, the antenna is held in place and transported on the cart by a small basket that lies slightly above the ground surface. This results in the recorded data carrying with it information regarding the separation between the antenna and the ground surface. This data must be removed to attain more accurate apparent depths to interfaces. To remove this data, the user must select the Time Zero option in either the Easy Processing tab or the Processing tab. This option is also located in the panel on the left of the screen under the Processing tab within Step 1. Once this option is selected, a wiggle trace will appear representing a recorded wavelet. The user simply adjusts this wiggle trace to line up with the first peak, thus removing the antenna-ground surface gap.

In most GPR surveys, background noise generated by diffractions, multiples, interference from other sources, and many other causes, are present in the recorded data. At the user's discretion, this data can be removed by selecting the Background Removal option present under the same tab(s) Time Zero is located under. If using the left panel, this option is located under Step 2. For this project, the Fullpass Filter was selected to remove specific frequencies and allow anomalies to be better viewed. After background noise was removed, the gain was changed to 6 to slightly increase the amplitude of the remaining signals.

3.3.3. Other Processing Options. The above steps were the only processing steps performed in this project. Within RADAN are many more processing steps that can be used to enhance the visual aspects of the data. In some cases, these remaining options are useful, but for this specific project, they were not necessary as they would only alter the data more than needed. Some useful processing steps not used are migration, horizontal scaling, vertical scaling, surface normalization, various filters, point picking for layer or rebar mapping, and many others. Point picking can be seen as interpretation and is used to create a file to be opened in Surfer software. This software allows for 3D and 2D profiles to be created.

4. TIME DOMAIN ELECTROMAGNETICS (TDEM)

4.1. BASIC THEORY

The time domain electromagnetics (TDEM) method operates in a way very similar to GPR. Much like GPR, TDEM uses electromagnetic (EM) pulses to measure properties of the subsurface. In the case of TDEM, however, the varying electrical conductivity is measured.

A transmitting coil is used to create a time varying magnetic field at the Earth's surface. This varying magnetic field generates a corresponding electrical field, which in turn creates an electric current that propagates through the underlying soil (French, 2002). This initial current will quickly decay until equilibrium is restored. If a metalliferous object is encountered by the propagating electric current, eddy currents are generated within the object, thus creating another electric field called the secondary electric field. By Faradays law of induction, a corresponding secondary magnetic field will be generated.

In the time frame between pulses, called the time-off, the secondary magnetic field is measured. These measurements occur at multiple time gates during this time frame, depending on the type of system used and the user's discretion. A graphic demonstrating this process is shown in Figure 4.1. Measuring the secondary current at multiple time gates during the time-off phase allows for analysis of decay of the magnetic field over time. When a secondary magnetic field is induced by a metalliferous object, the measured magnetic field at that location will appear as an anomalous measurement as a spike. Comparing these measurements provides information on the variance in

conductivity of the underlying soil or layers and give information about buried metal objects. More conductive materials will allow the electric current to travel further, while more resistive materials will cause the electric current to decay more rapidly.

Propagating electric currents tend to spread out as they travel further from the source pulse. Directly under the transmitter antenna, the current will be very small. As the current propagates through the subsurface, it will spread out through diffusion. This spreading and diffusing results in weakening of the current. This causes the measured magnetic fields from deeper interfaces to be weaker than the shallower interfaces.

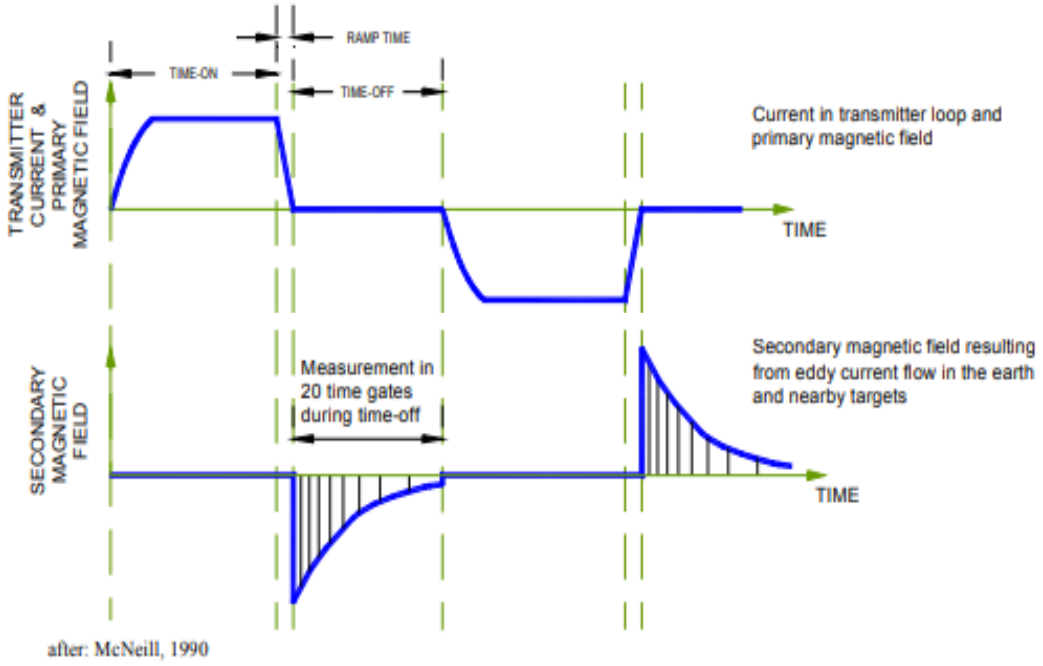

Figure 4.1: Original current (top) and measured secondary current (bottom).

There are many TDEM units that are mobile and used as metal detectors. When metalliferous objects are encountered by a propagating electric current, the ions are excited and eddy currents are generated. This response creates the secondary electric and magnetic fields recorded by the TDEM metal detectors, as seen in Figure 4.2. However,

when a mobile TDEM metal detector is used, the transmitter and the receiver are at the same location on the ground surface. This process allows the TDEM method to be used for rapidly locating buried objects such as underground storage tanks, munitions, or other objects of archaeological importance.

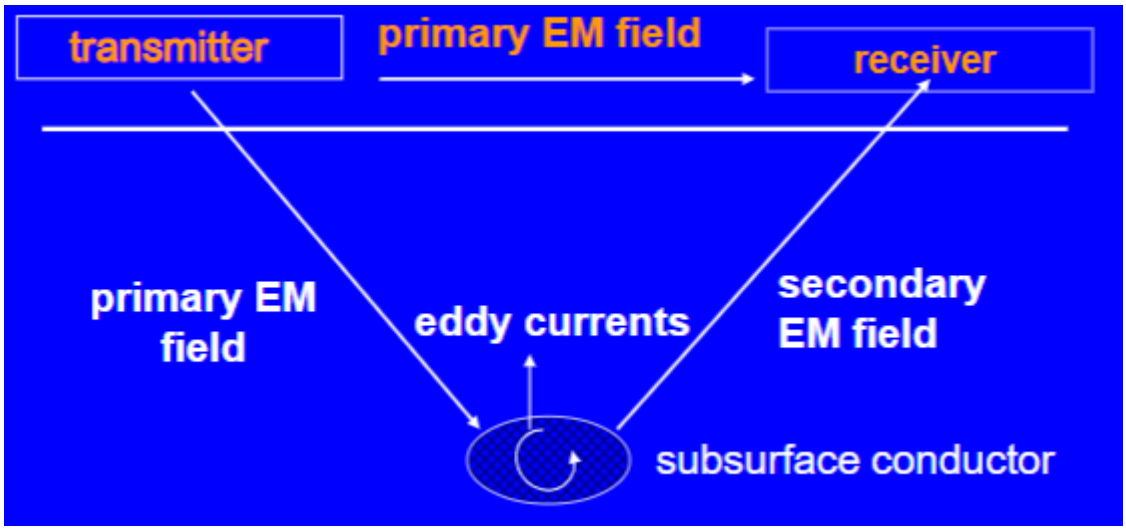

Figure 4.2: Flow path of electric current through a medium.

4.2. DATA ACQUISITION

Time domain electromagnetic data was acquired at the Big Blue Battlefield site with the Geonics Limited EM61-MK2A time domain metal detector. The EM61-MK2A allows for data acquisition in the time domain using four time gates. Time domain electromagnetic data was acquired along the same 36 west-east traverses that the GPR data was acquired along at Site A. Time domain data was only acquired at Site A. According to Daniel Smith, the entirety of the Big Blue Battlefield site, specifically the locations of Site B and Site C, has been investigated by countless individuals trying to

acquire artifacts for their personal collections. Site B and Site C have also been more heavily excavated for industrial uses, with Site C being littered with utility lines.

4.2.1. TDEM Antenna Set Up. The EM61-MK2A is transported in two separate boxes. One contains the wheels and batteries and the other box contains the two coils and the U-handle. Each of the coils are rectangular and measure one meter wide and half a meter long. The coils are connected to each other at each corner by 30cm vertical bars and are connected at the site. The upper coil is a receiving coil used for focusing and the lower coil doubles as the EM source as well as the main receiving coil. The U-handle, which holds the electronics console, is connected to the back of the unit adjacent to the lower coil. The two wheels are attached at either side of the unit and the battery is placed in the center of the lower coil (Figure 4.3).

Figure 4.3: Geonics Limited EM61-MK2A.

4.2.2. Data Acquisition. After the TDEM unit was set up, acquisition began. Data were acquired along 36 parallel traverses oriented west-east at Site A. The paths left from

the wheels during GPR data acquisition were followed. This allowed rapid acquisition of data along all 36 traverses. Much like the GPR acquisition process, the first traverse was oriented west to east, the second east to west, and so on. After acquisition of each traverse, a new file was created to denote the opposing direction. The large and small concrete slabs in the southwest corner of Site A resulted in gaps in the TDEM data acquisition process.

During the acquisition process, data is shown in real time on the control unit for in field interpretation. This allowed for field notes of anomalies to be recorded during acquisition, as well as letting the user know that the unit was working properly. Once all the 36 profiles were recorded, an extra profile was recorded at the northeast corner of the site extending towards the road. This was done to test the orientation of prominent anomalies along the northern boundary of Site A.

4.4. DATA PROCESSING

Processing of TDEM data for this site is fairly straight forward and quickly turns into interpretation. First, a notepad version of the data is opened and inspected visually for anomalies. Every other file is reversed so that the orientations of each file match. The data file is then uploaded to the DAT61MK2 software, the specific software provided by Geonics for processing data acquired by the EM61-MK2 acquisition system. Here, the user can select which time gate or time gates to use and convert the data to be used in other software. Both of these tools were utilized in the processing step for this project, Once done, the data was extracted and uploaded onto Surfer Software for plan view profile creation and interpretation.

5. FREQUENCY DOMAIN ELECTROMAGNETICS (FDEM)

5.1. BASIC THEORY

Much like the TDEM method, the frequency domain electromagnetics method, or FDEM method, uses electromagnetic energy to detect variations in conductivity in the subsurface. The FDEM method, however, operates at specified frequencies and does not measure the decay rate of the secondary currents. The FDEM method also continually transmits electromagnetic energy, as well as receives it. The transmitted energy propagates as a sinusoidally varying current. When this energy meets a conductor in the subsurface, the conductor will produce a secondary current that is out of phase with the transmitted current. The receiving antenna constantly measures the total magnetic field. When the secondary current is recorded, the recorded total magnetic field increases and the unit chimes to signal the user that a metalliferous object is present.

5.2. DATA ACQUISITON

Acquisition of frequency domain electromagnetics data was performed post processing of the GPR and TDEM data. The results from the GPR and TDEM data, specifically from the TDEM data, presented areas of interest for further investigation. In total, there were eight areas of interest located on the TDEM anomaly map. The GPS coordinates of these locations were extracted from Google Earth to be used in the field to find exact locations. A handheld GPS was then used, along with visual estimations of locations, to find the locations of these areas of interest while in the field. Once a location

was believed to be found, an FDEM metal detector was used to locate the exact spot for excavation and a shovel was used to extract the buried object.

The FDEM metal detectors JW Fishers Pulse 8x (Figure 5.1) and the Radio Shack Discovery 3000 (Figure 5.2) were brought to the field for acquisition purposes. The JW Fishers Pulse 8x metal detector has three sensitivity settings, low, medium, and high. The high sensitivity setting is used to locate a general area that an object is in. The medium and low settings are then used to pinpoint the exact location. This metal detector also provides the audio output to be listened to with a pair of earphones, making it easier to hear. The Discovery 3000 metal detector has four target modifications, All Metal, Disc (discrimination), Notch, and Auto Notch. Various types of metals are ignored based on whether Disc, Notch, or Auto Notch are selected. If All Metal is selected, all types of metal will be recognized. Both units are handheld metal detectors consisting of two coils. The transmitting coil which is the outer coil, and the receiving coil which is the inner coil.

Figure 5.1: JW Fishers Pulse 8x metal detector.

Figure 5.2: Radio Shack Discovery 3000 FDEM unit.

To locate buried metal objects, the user holds the unit above the ground surface and moves it in a swaying motion to the left and right. When a metal object is below the unit, a tone is sounded, and the display shows what type of metal is present. To find the objects exact horizontal location, the user must find the boundaries where the signal will be recorded. This usually gives a circular area that holds the buried object. Repeating this process in narrowing circles will show the exact location. If the signals from all locations surrounding the metalliferous object were to be displayed, a large bowl-shaped detection area would be visible (Figure 5.3). After the exact location was found, a shovel was used to dig up the buried object. Though depths can be estimated by the detection area, exact depths to objects are unknown until they are located through excavation.

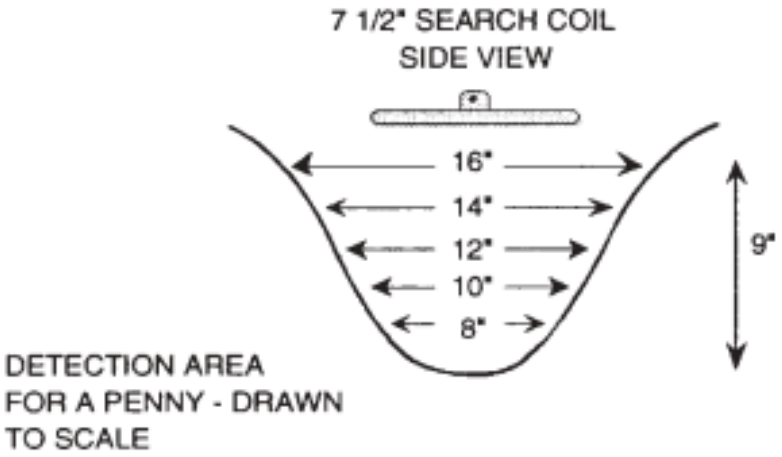

Figure 5.3: Bowl shaped detection area for a penny (Pulse 8x Operation Manual).

6. INTERPRETATION AND RESULTS

6.1. GPR DISCUSSION

6.1.1. GPR Interpretation. Each of the 2D GPR traverse profile images were aligned using PowerPoint to see if a continuous anomaly representative of a road had been recorded. In doing this, two continuous anomalies were found. One of these were at Site A (Figure 6.1-6.5). Another continuous anomaly appeared at Site B (Figure 6.6). All GPR traverse profiles for Site A are displayed in Appendix A. The GPR traverse profiles from Site B and Site C are displayed in Appendix B.

6.1.1.1. Site A anomalies. The continuous anomaly found at Site A can be seen on traverse profiles 34-36 and is indicated by the red rectangle on Figure 6.1. This same anomaly is seen in traverse profiles 37-50 (Figures 6.2-6.5).

Figure 6.1 shows anomalies on traverse profiles 36, 35, and 34. On each of these profiles, the anomaly appears as a high amplitude reflection at depths ranging from one foot to one and a half feet. The anomaly on the profile for traverse 36 is approximately 50 feet in length. The anomaly on the profile for traverse 35 is approximately 70 feet in length. The anomaly on the profile for traverse 34 is approximately 15 feet in length.

Figures 6.2 to 6.5 show anomalies on traverse profiles 37 to 51. Each of these anomalies appear as high amplitude reflections at a depths less than one foot on the north end of the profiles. The anomalies of traverse profiles 37-42 are approximately 20 feet in length. Anomalies on traverse profiles 43-53 become shorter until they are no longer visible.

When the locations of these high amplitude reflections are compared to the lineaments seen on Figure 6.7, it is clear that the recorded anomalies coincide with the visible lineaments present in the field.

6.1.1.2. Site B anomaly. Site B contained a continuous anomaly that appeared on each of the four GPR profiles collected here. This anomaly is oriented west to east making it easily visible in the north to south traverse profiles and is shown in Figure 6.6. Each of these anomalies appear as high amplitude reflections at depths ranging from one foot to two feet. In the profile for traverse 1, the anomaly is mostly flat and not as prominent as the reflections seen in the profiles for traverses 2, 3, and 4. The anomalies that appear in the profiles for traverses 2, 3, and 4 begin at a depth of two feet at the 35 foot mark. Each of these appear as a flat reflection surface for 6 feet, where the reflection surface rises to a depth of one foot.

6.1.2. Results. The anomalies presented in these traverse profiles would likely indicate that the buried road was in fact imaged. However, upon observing historical maps from 1963 and 1990 presented by Daniel Smith and available on Google Earth it is evident that there is a distinct path, belonging to the previously existing railway, adjacent to the parking lot and roadway. This relationship is shown in Figure 6.7 below and was used to determine that the anomalies highlighted along the north end of Site A were due to the old railroad spurs. These images also show that the anomalies seen along the traverse profiles from Site B could be due to the railroad spurs as well, but according to Daniel Smith there was a recent excavation in this area, which is likely in reference to the excavation of the railroad spur. According to Daniel Smith, the railroad spurs were set up

just after the 1963 image he provided us and were removed in 1989 when his group acquired the site, just prior to the image taken from Google Earth.

Further, there appears to be banks at the ends of each anomaly, separated by a flat region that would be the base, indicative of an excavation. This is likely due to the excavation of the previously existing railroad ballasts. The presence of the railroad spur through the northern portion of the site likely caused compaction of the underlying soils. These compacted soils could be the cause of the high amplitude reflections discussed here. If this is not the case, then the dielectric properties of the soils used to infill the excavation must vary from those of the dielectric properties of the native soils.

In addition to these historical maps disproving that these anomalies could be caused by the historic Byram's Ford Road, the widths of these anomalies can be taken into consideration. Since Byram's Ford Road was used to transport supplies, it is likely that the wagons carrying these supplies would match the plans presented in the Antique Ordinance Publishers plan for the typical model 1858 six-mule supply wagon used in the Civil War. This document states that axles of these wagons were approximately 4 feet in width. If the paths from the wagon wheels were the only trace of Byram's Ford Road left, the resulting anomaly would appear as two high amplitude reflections approximately 4 feet apart. As described above, these anomalies are much wider than 4 feet and are continuous reflection surfaces.

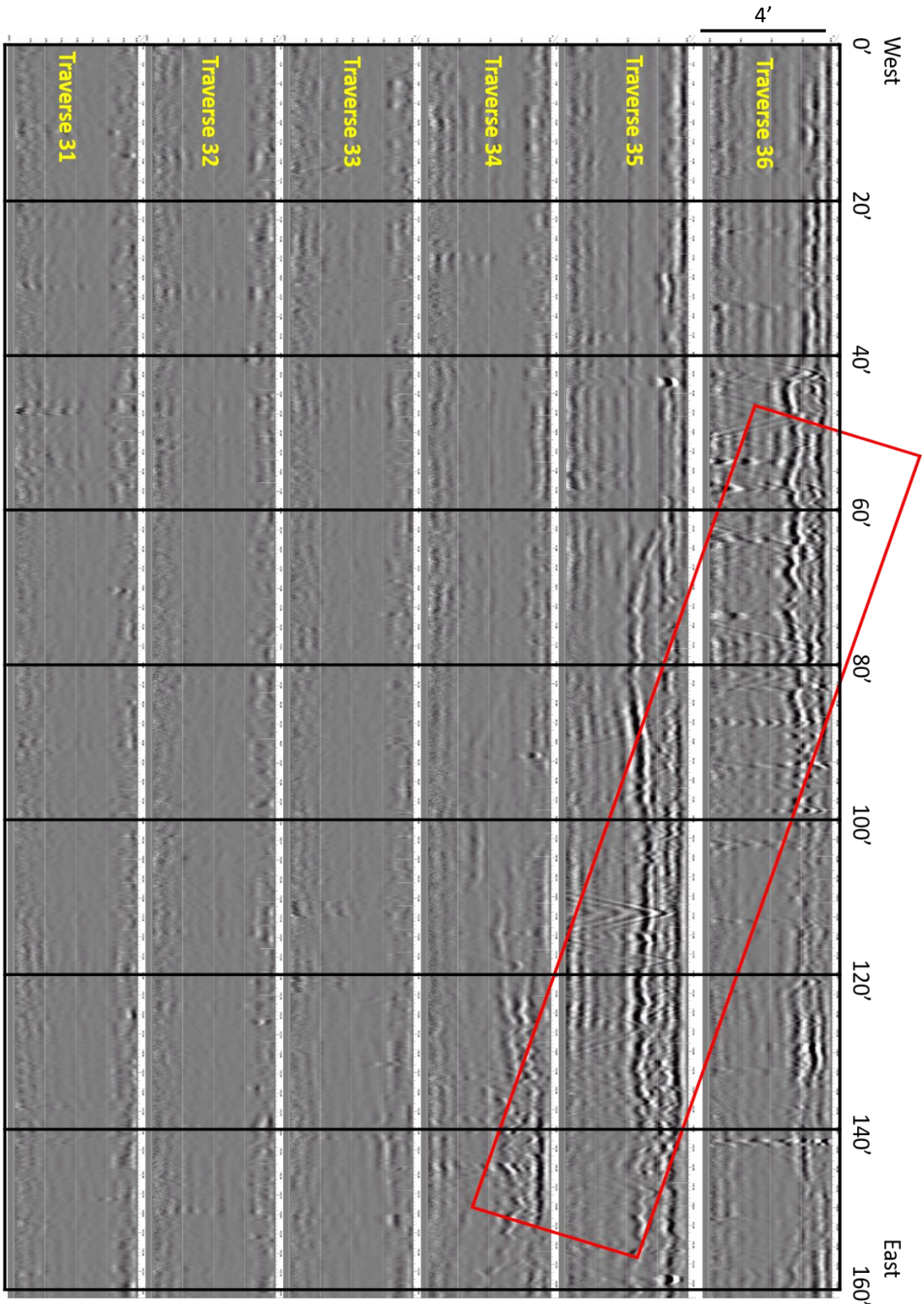

Figure 6.1: GPR profiles for traverses 31-36 with railroad spur anomalies indicated.

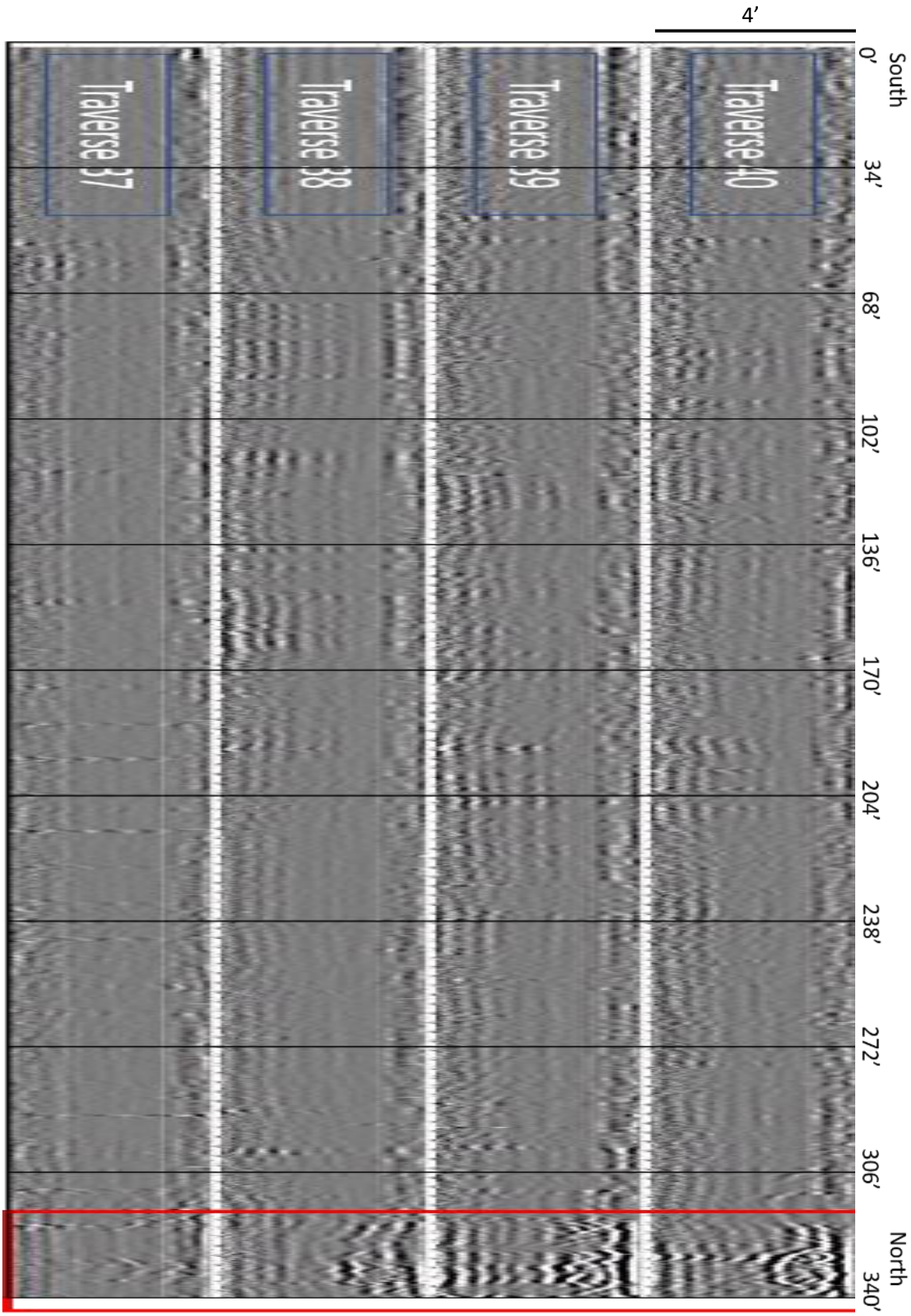

Figure 6.2: GPR profiles for traverses 37-40 with railroad spur anomalies indicated.

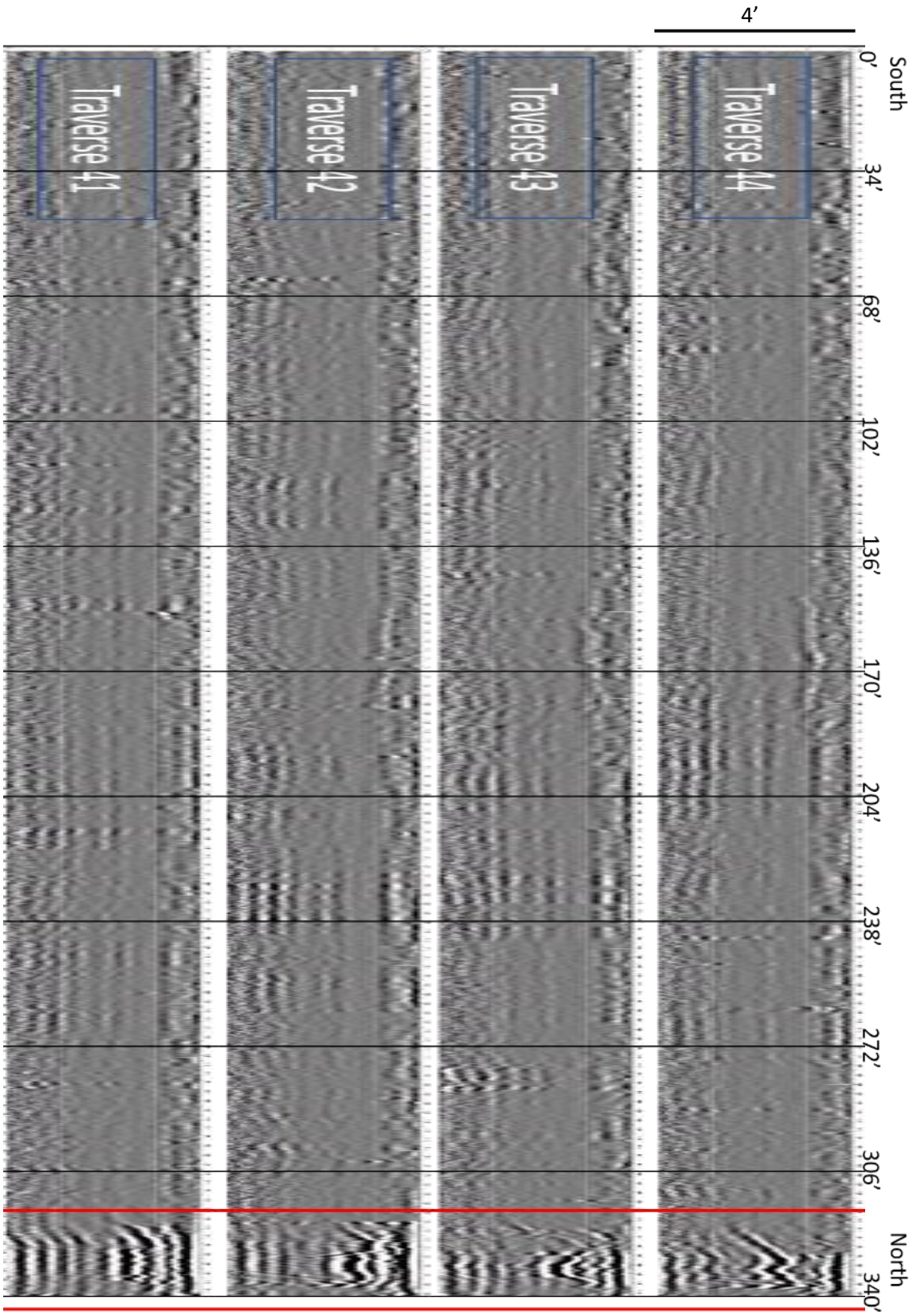

Figure 6.3: GPR profiles for traverses 41-44 with railroad spur anomalies indicated.

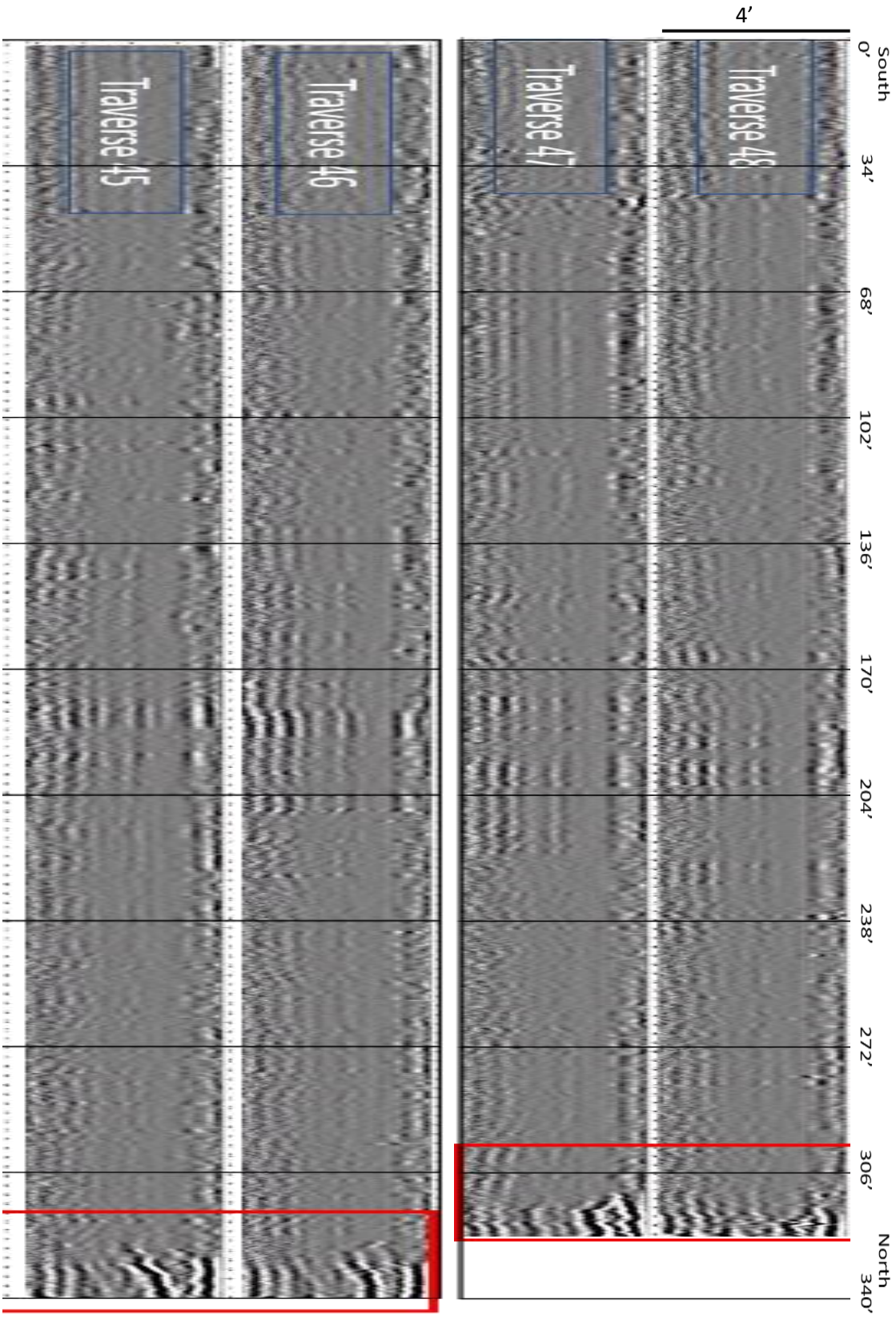

Figure 6.4: GPR profiles for traverses 45-48 with railroad spur anomalies indicated.

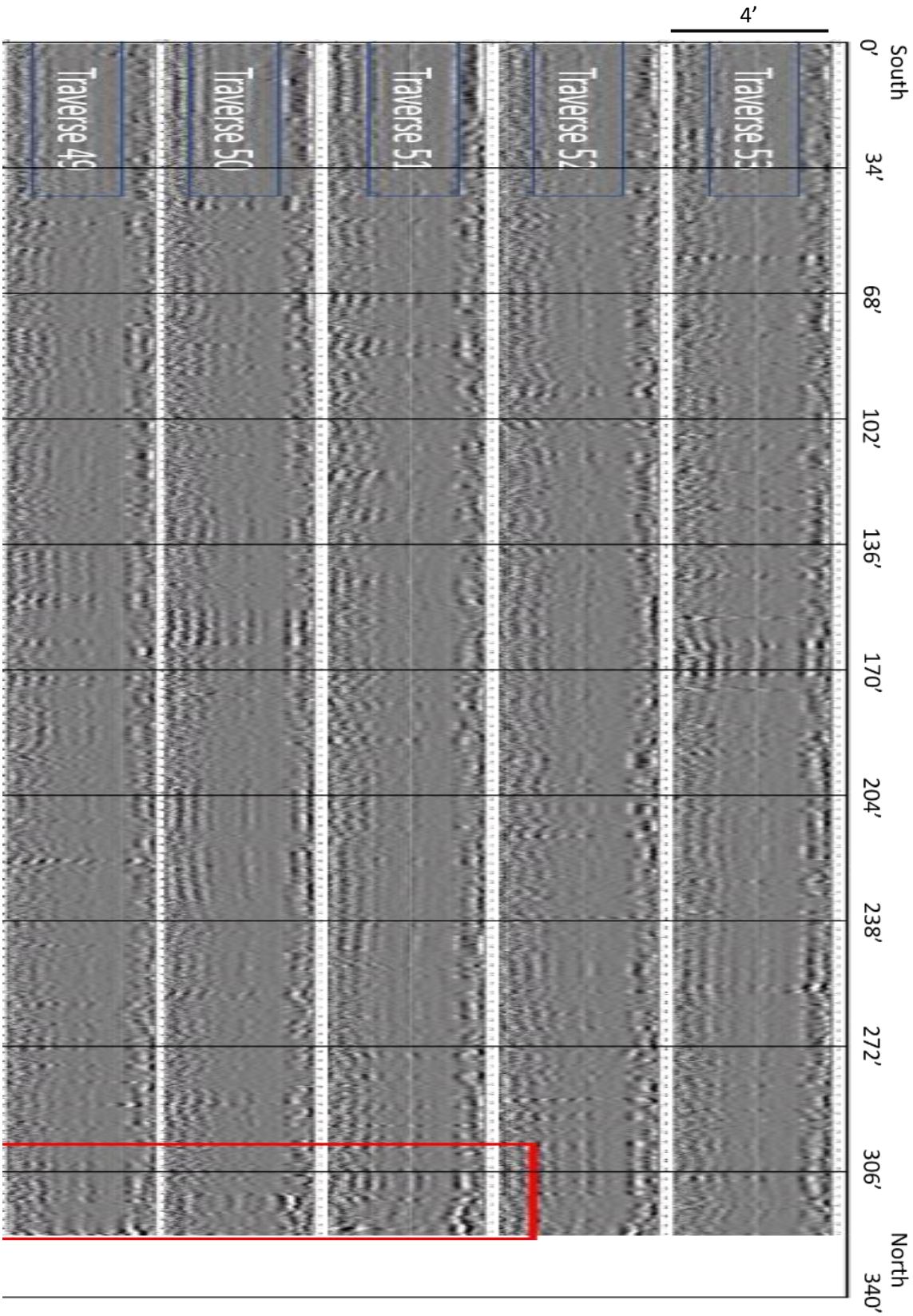

Figure 6.5: GPR profiles for traverses 49-53 with railroad spur anomalies indicated.

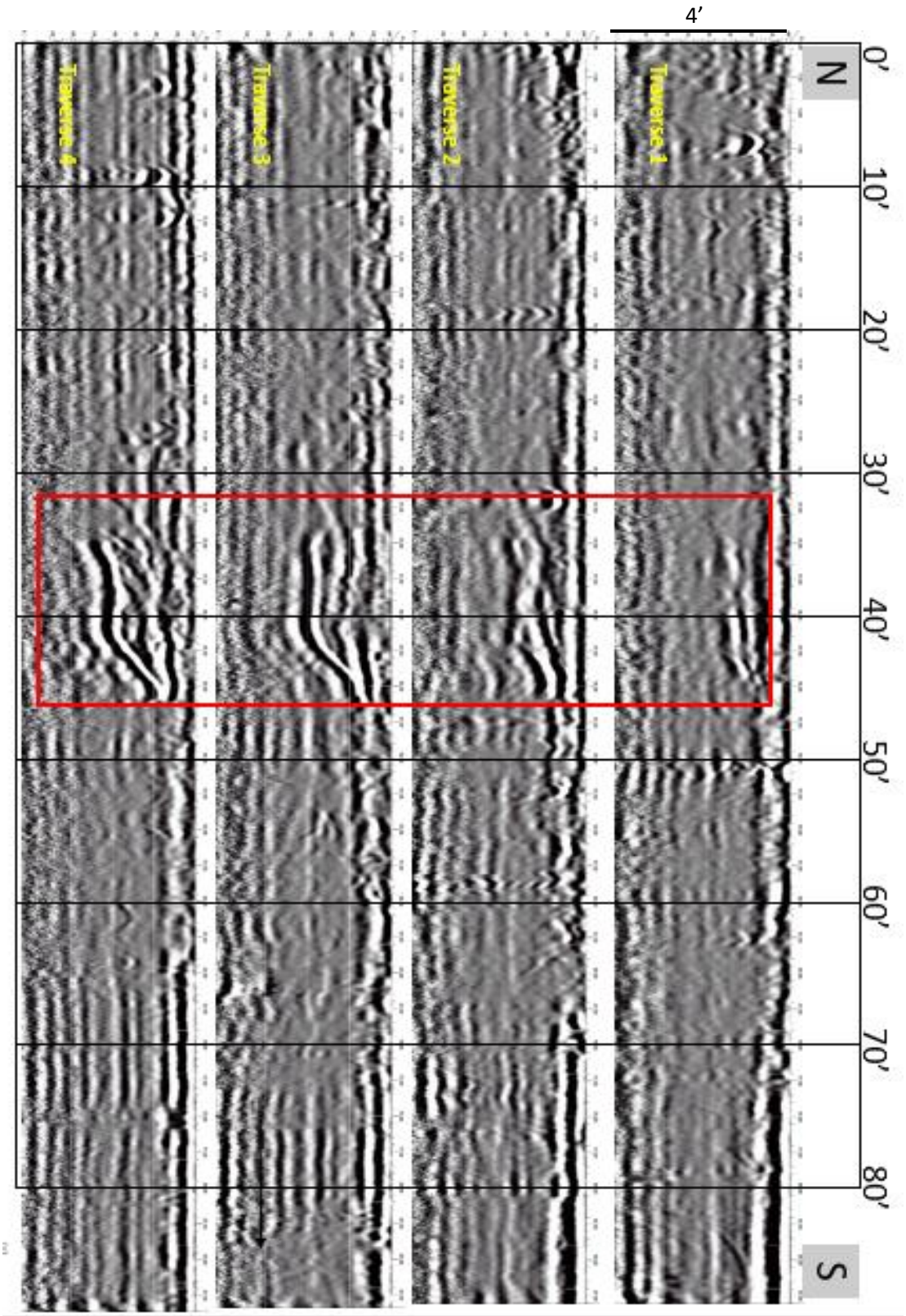

Figure 6.6: GPR profiles for traverses 1-4 from Site B. Red rectangle shows prominent anomalies.

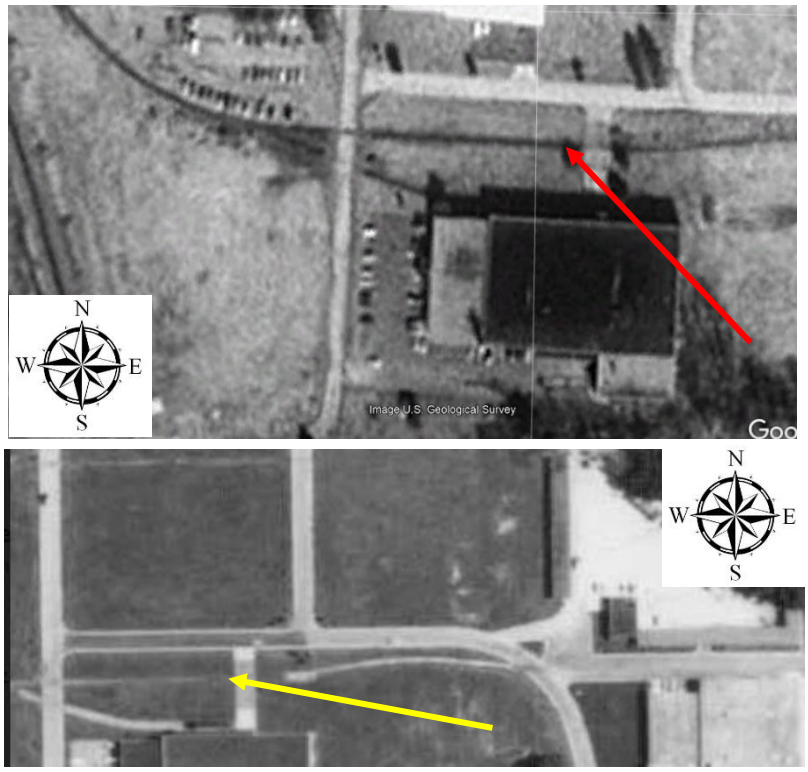

Figure 6.7: Top image taken from Google Earth, 1990 image by USGS showing where railroad spurs were in the study area (red arrow). Bottom image provided by Daniel Smith from 1963, with a similar path (yellow arrow) to the north of the building. Both arrows point to the same location.

6.2. TDEM DISCUSSION: INTERPRETATION AND RESULTS

Data extracted from TDEM processing was uploaded to Surfer Software for interpretation. Uploading this data to Surfer allowed for a 2D plan view profile to be created of Site A (Figure 6.8). This 2D plan view image of the data revealed multiple anomalies. These anomalies can be split into three groups: possible railroad spurs (red rectangle), unknown (yellow rectangle), and the large and small concrete slabs and accompanying piping (green rectangle).

Since it was already known that there were railroad spurs intersecting the site on the north end which also appeared in the GPR data, and the gaps in the data due to the concrete slabs resulting in high millivolts response, these areas were excluded from further investigation. This left the area of unknown to be investigated. The relatively high response along the east and south edge of Site A are due to the small flags used to mark traverse location. This was done using FDEM.

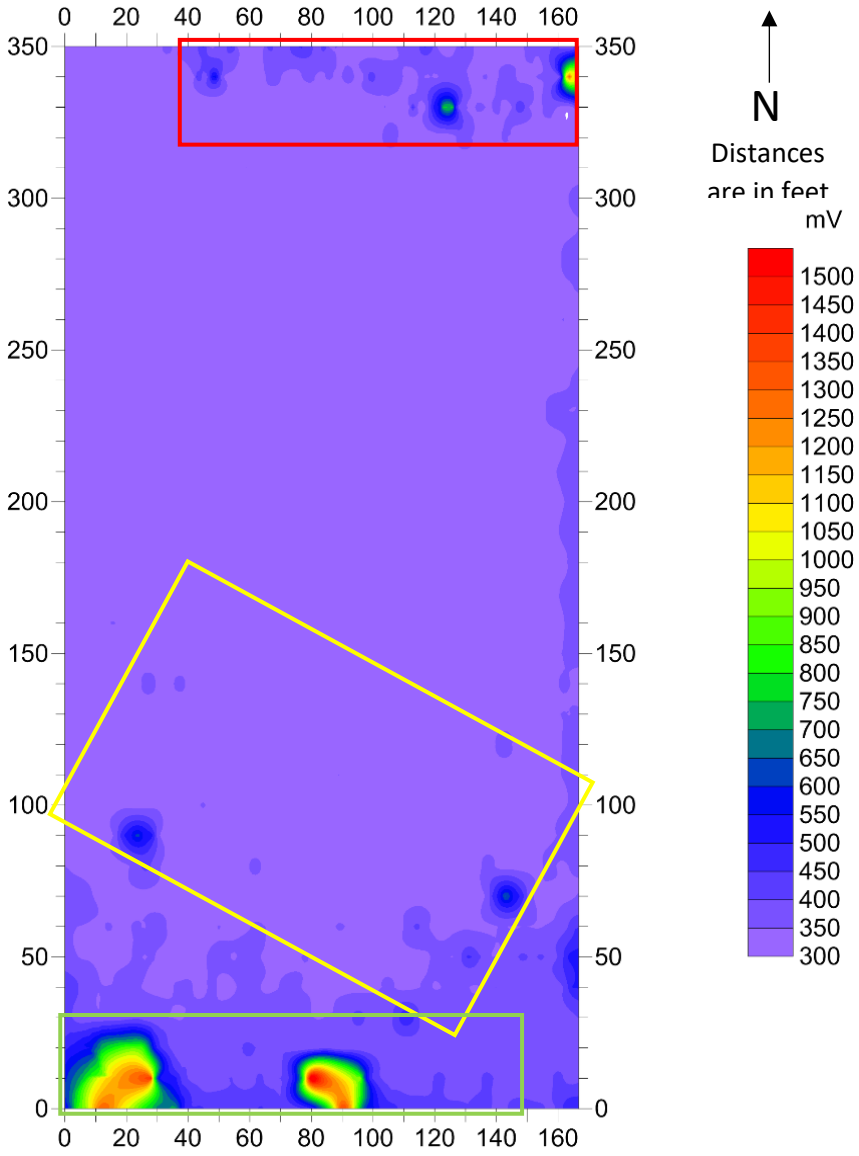

Figure 6.8: TDEM Site A profile.

6.3. FDEM DISCUSSION

Data acquired with the FDEM method were interpreted in field with the assistance of Daniel Smith. His extensive knowledge of the battle and land uses between then and the present made for reliable interpretation of the significance of all objects recovered. There were many anomalies present in the area of interest, only eight of which maintained any significance. Their locations are shown in Figure 6.9 and the objects found at each location are shown in Figure 6.10. Many other anomalies were investigation, but only litter was found. In two locations, recently distributed Busch Light cans were excavated at depths greater than 2 inches. These depths indicate that the area has a relatively high deposition rate.

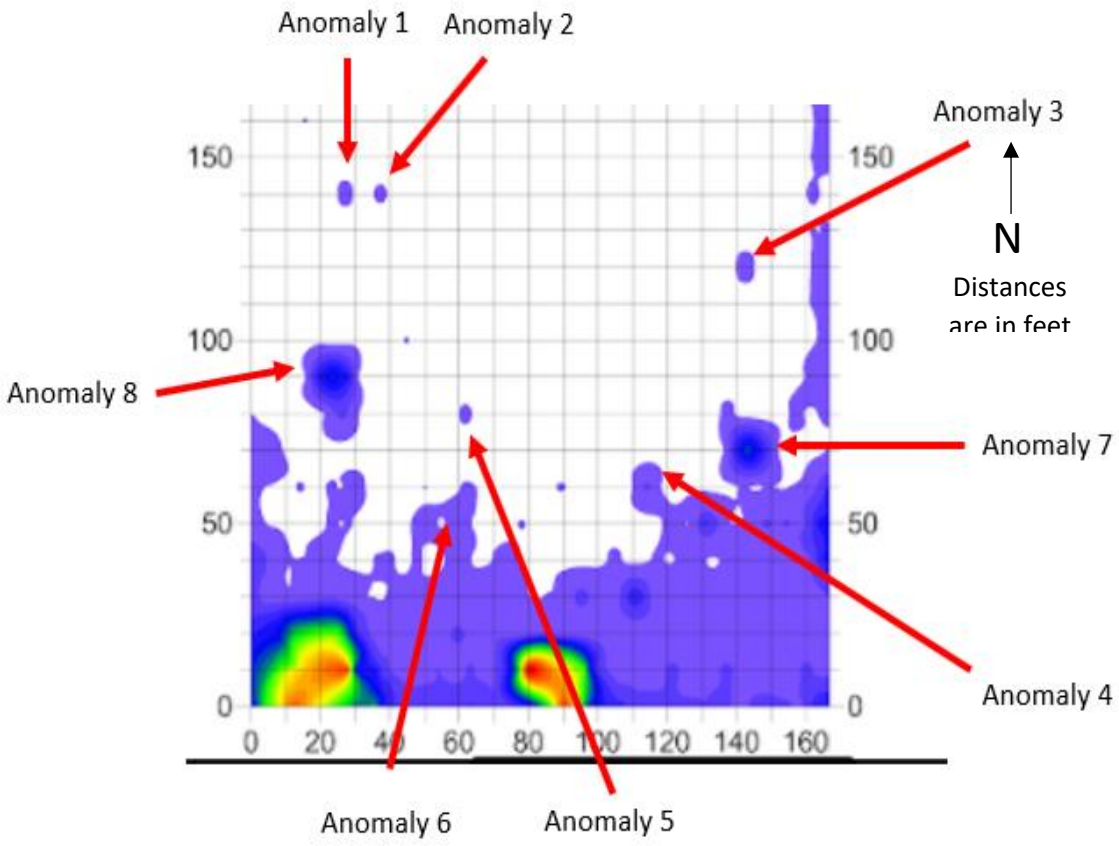

Figure 6.9: Anomaly 1-8 locations.

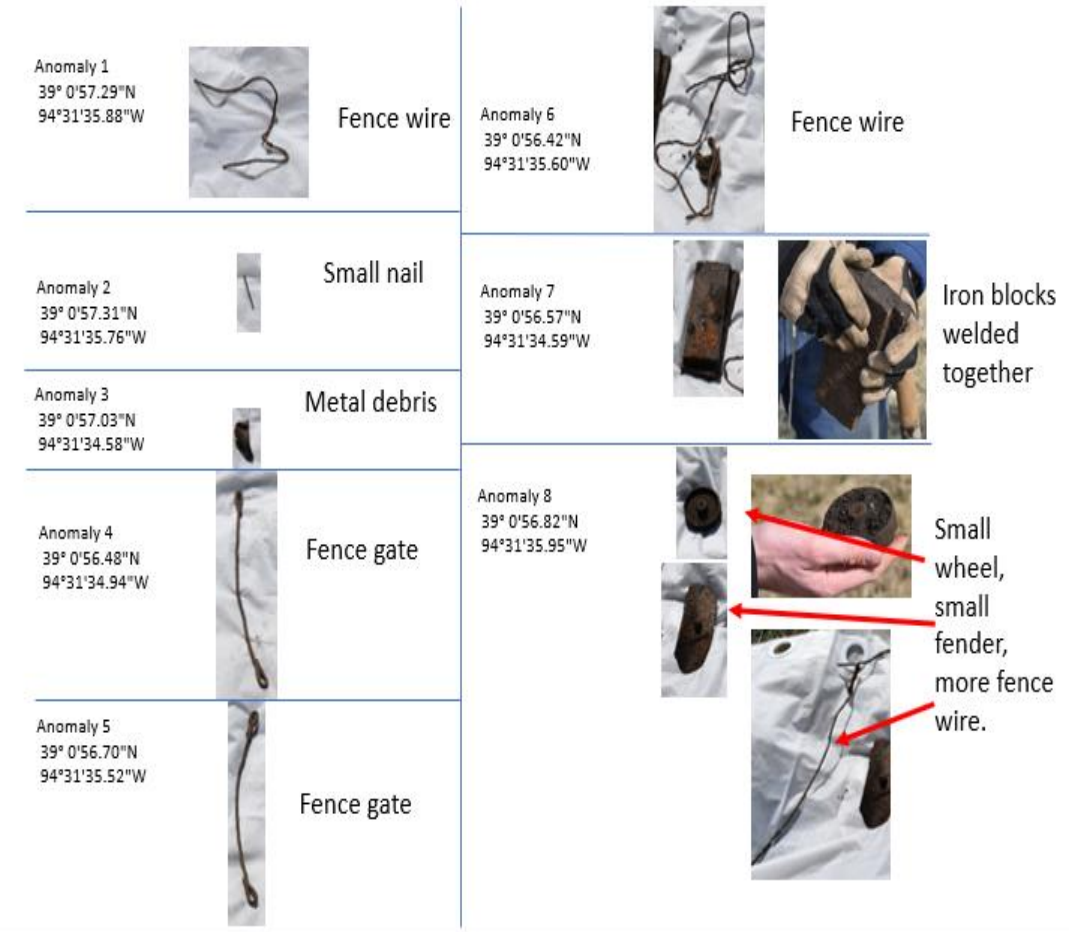

Figure 6.10: Each anomaly and their corresponding object(s).

According to Daniel Smith, this site has had multiple uses since the day of the battle in 1864. One of the main uses for this land was as a small farm. Daniel Smith speculates that Site A was fenced in, which is why many metal pieces resembling parts of a wire fence (anomalies 1, 4, 5, 6, and 8) were found. The small nail found at anomaly 2 and small wheel and fender found at anomaly 8 can also be attributed to the small farm. The metal debris at anomaly 3 and iron blocks at anomaly 7 have an unknown origin, but cannot likely be attributed to the battle.

7. CONCLUSIONS

The objective of this investigation was to locate a missing section of Byram's Ford Road believed to be dissecting the historic Big Blue Battlefield. The goal was to find this section using ground penetrating radar, a time domain electromagnetic metal detector and a frequency domain metal detector.

Geophysical data at three sites, Site A, Site B, and Site C, within the Big Blue Battlefield area were acquired. Though meticulous data acquisition and interpretation methods were employed, any possible location of Byram's Ford Road was disproven with the knowledge of the site history. Anomalies that appeared on the ground penetrating radar data at Site A and Site B as continuous high amplitude reflections spanning approximately 10 to 15 feet appear to be caused by the infilling of soils along the excavated railroad spurs that were placed in 1964 and removed in 1989.

Anomalies seen at Site C are localized hyperbolic signatures and are caused by buried electrical or pipe lines that the adjacent building uses. Localized anomalies seen on the time domain electromagnetic data for Site A were investigated using a frequency domain electromagnetic metal detector in the hopes that Civil War artifacts would be found. All excavated artifacts were identified as farm equipment, and none were thought to be from the Civil War.

Since this site has been used as a farm, once had a railroad dissecting it, apparently can have a high sediment deposition rate, and is currently being used as an industrial park, it is likely that this site has been disturbed too greatly through the course of history to correctly identify the missing portion of Byram's Ford Road.

APPENDIX A.

GPR TRAVERSE PROFILES FROM SITE A: 1-53.

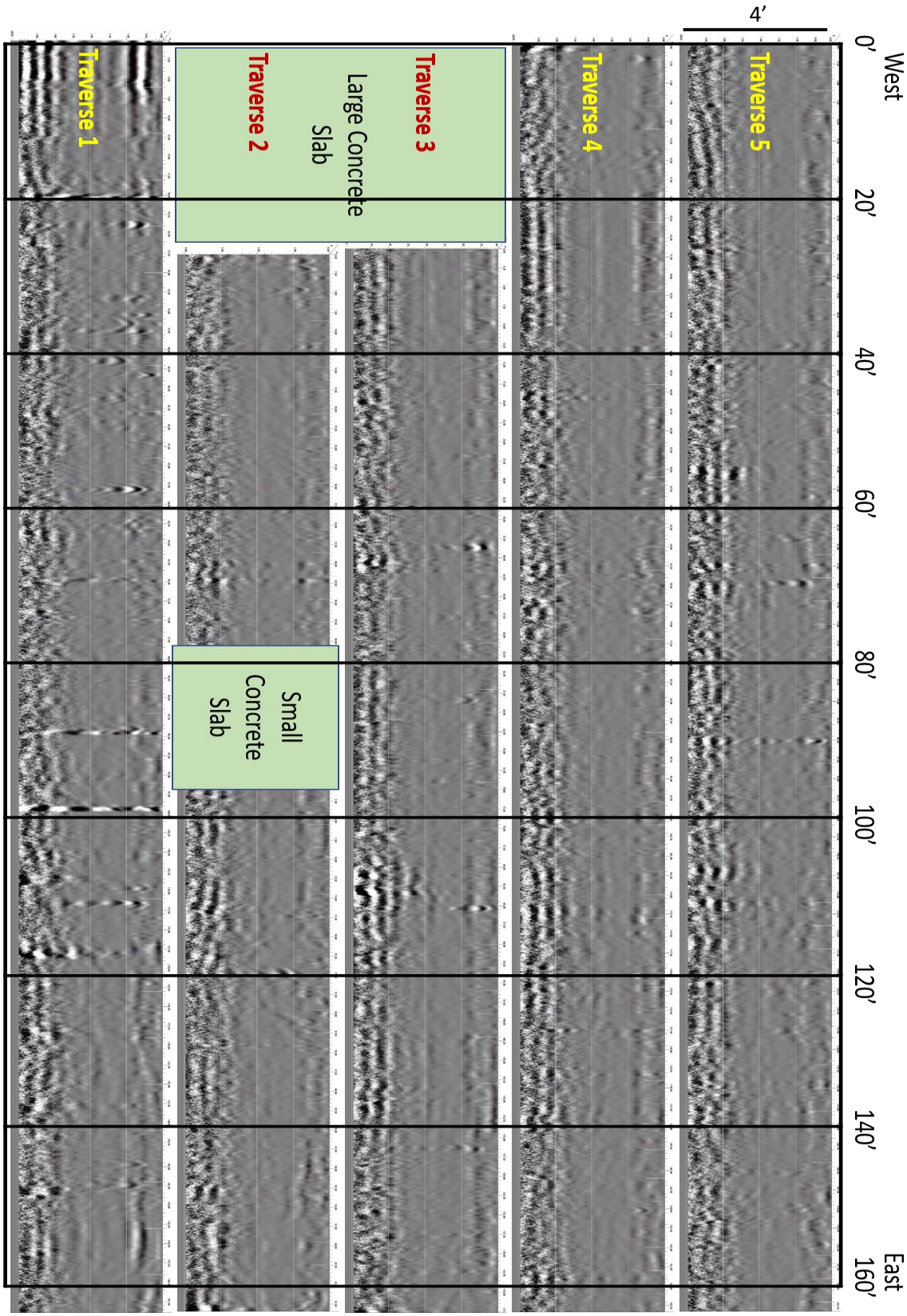

Figure A.1: GPR profiles for traverses 1-5 at Site A.

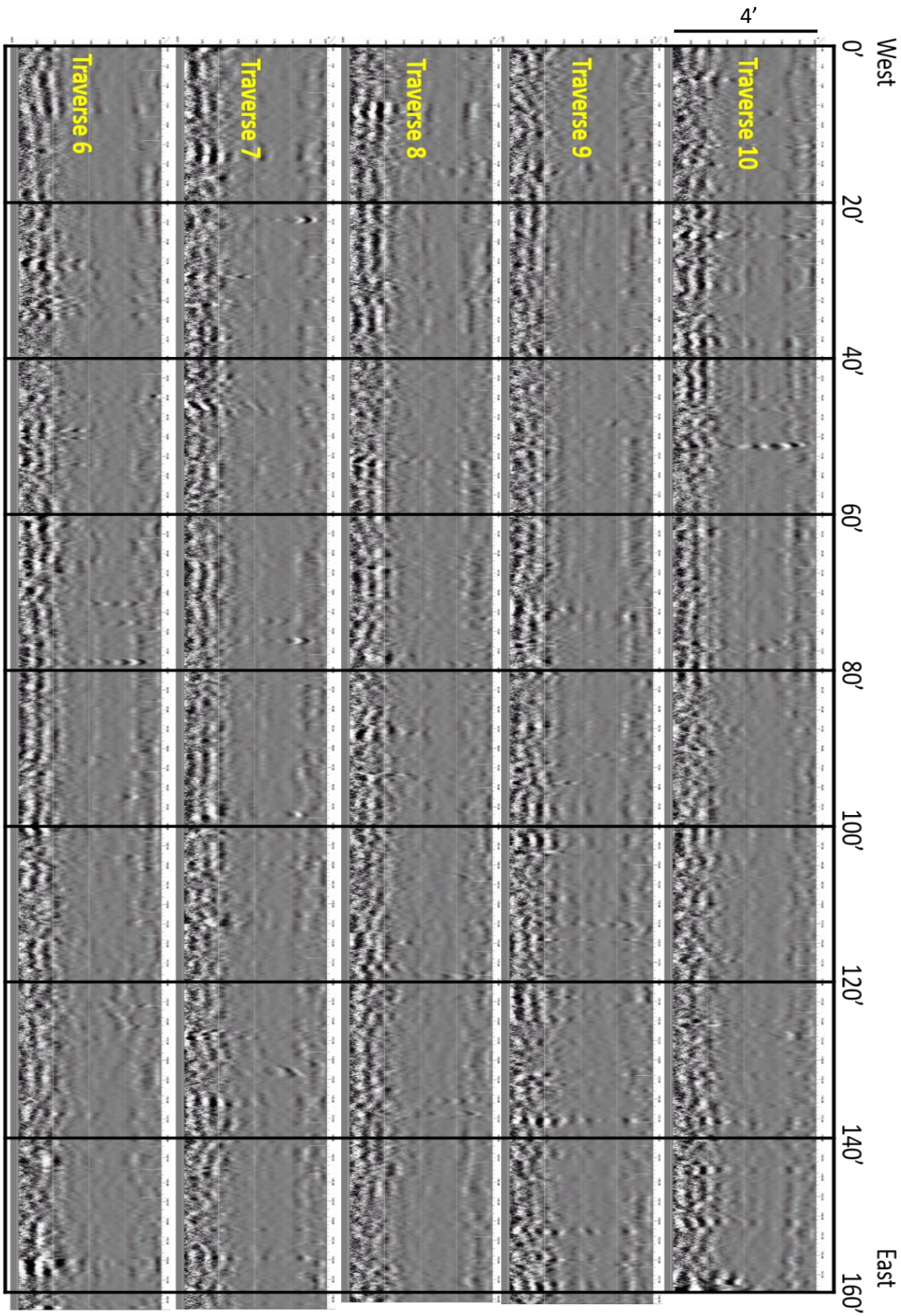

Figure A.2: GPR profiles for traverses 6-10 at Site A.

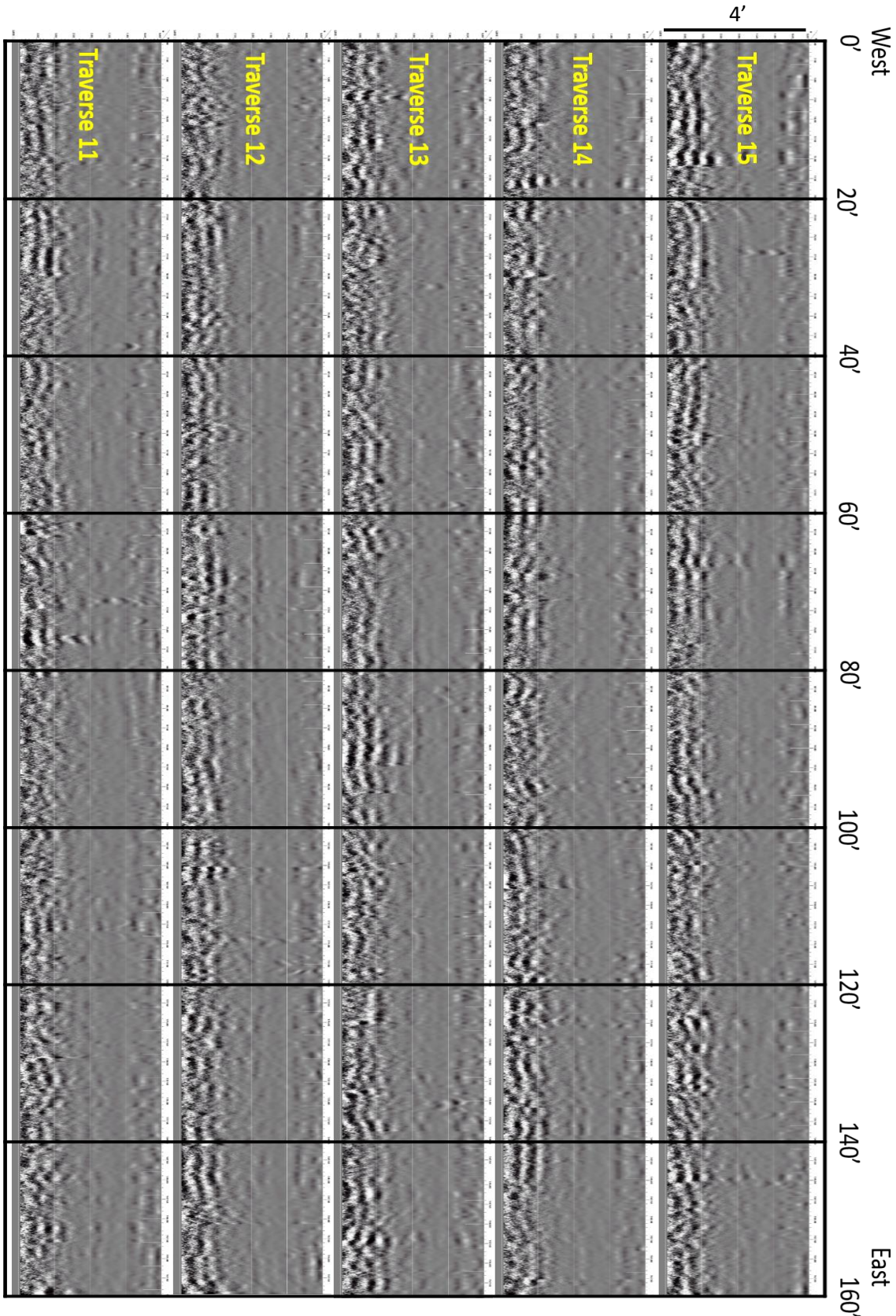

Figure A.3: GPR profiles for traverses 11-15 at Site A.

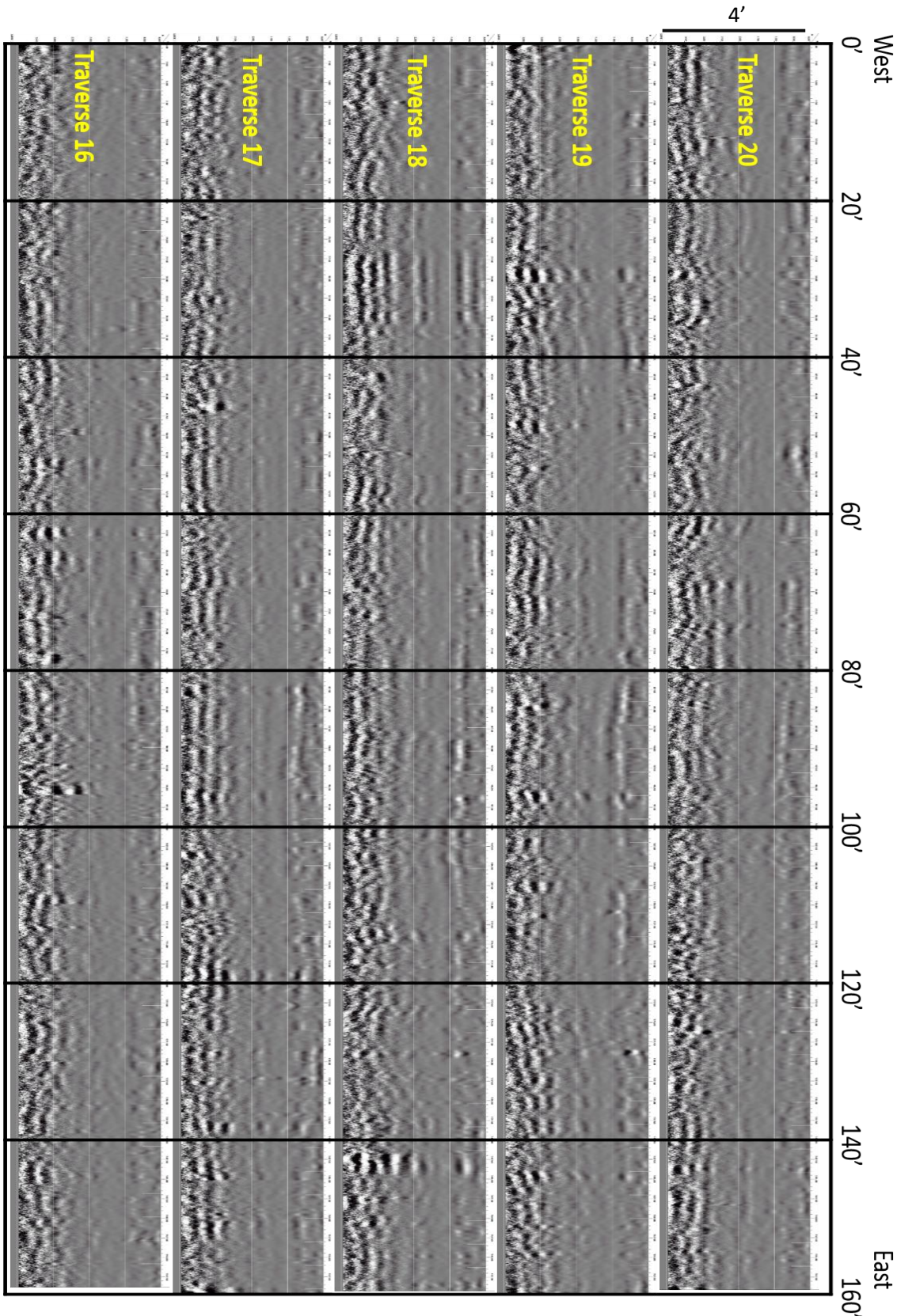

Figure A.4: GPR profiles for traverses 16-20 at Site A

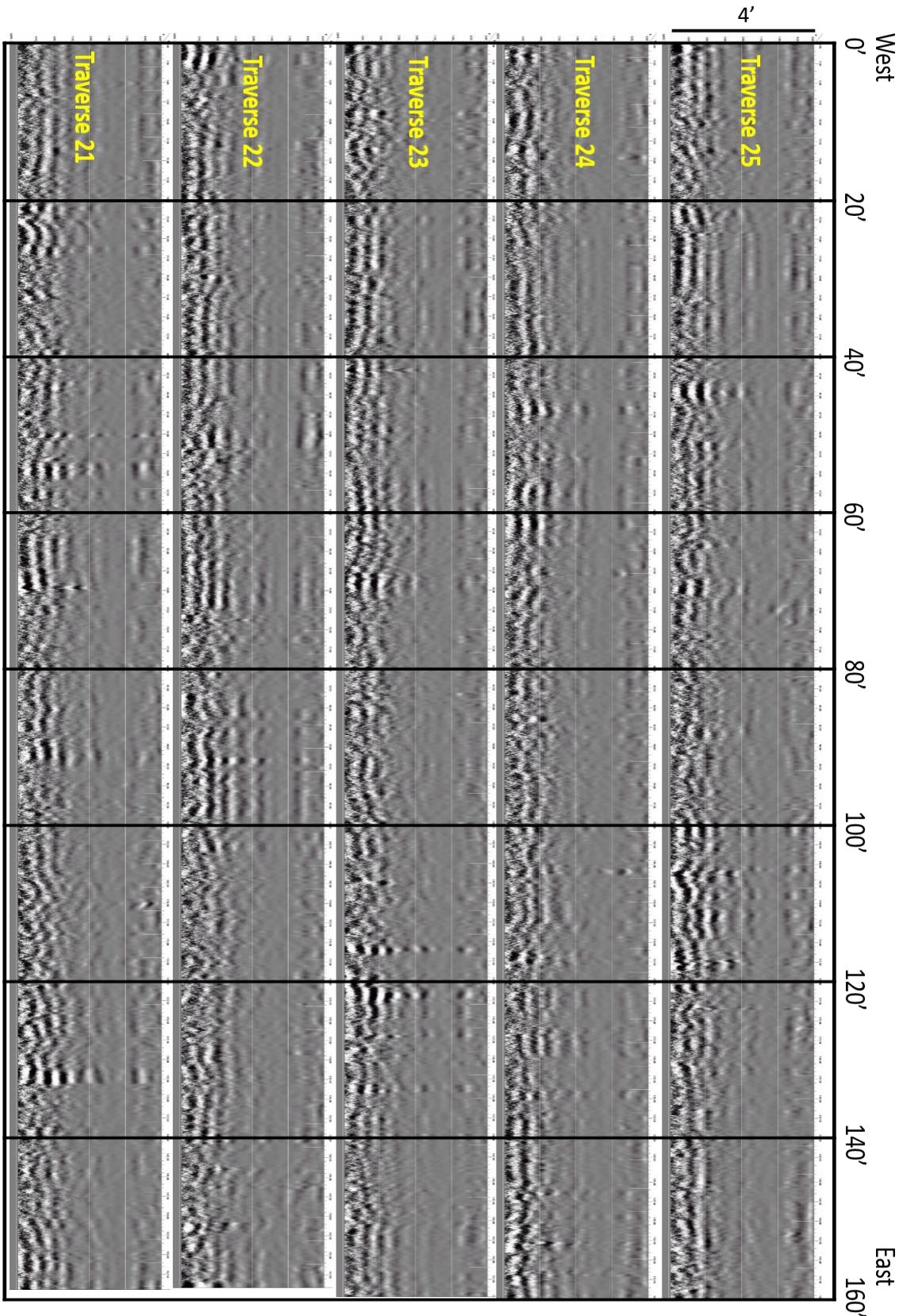

Figure A.5: GPR profiles for traverses 21-25 at Site A.

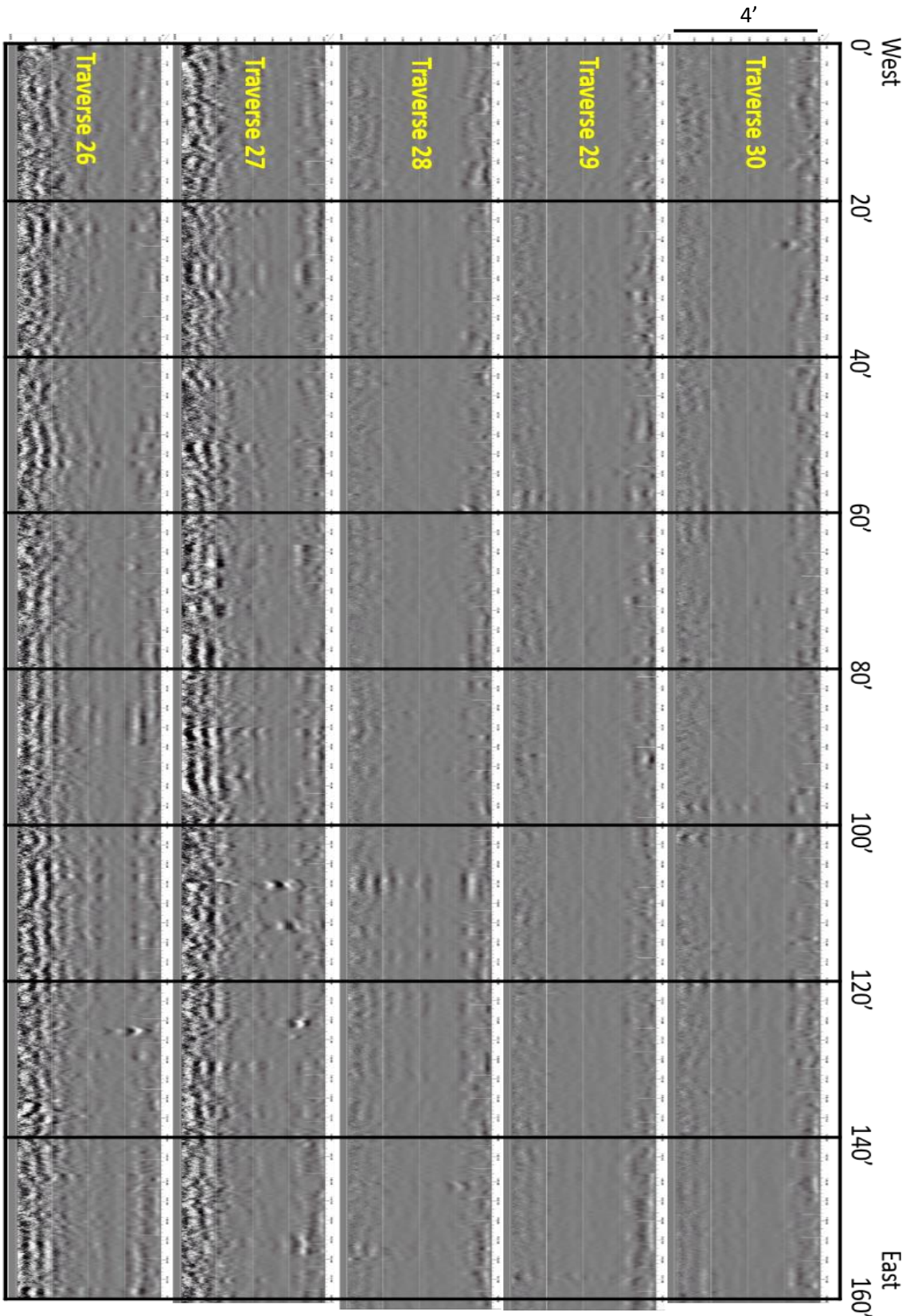

Figure A.6: GPR profiles for traverses 26-30 at Site A.

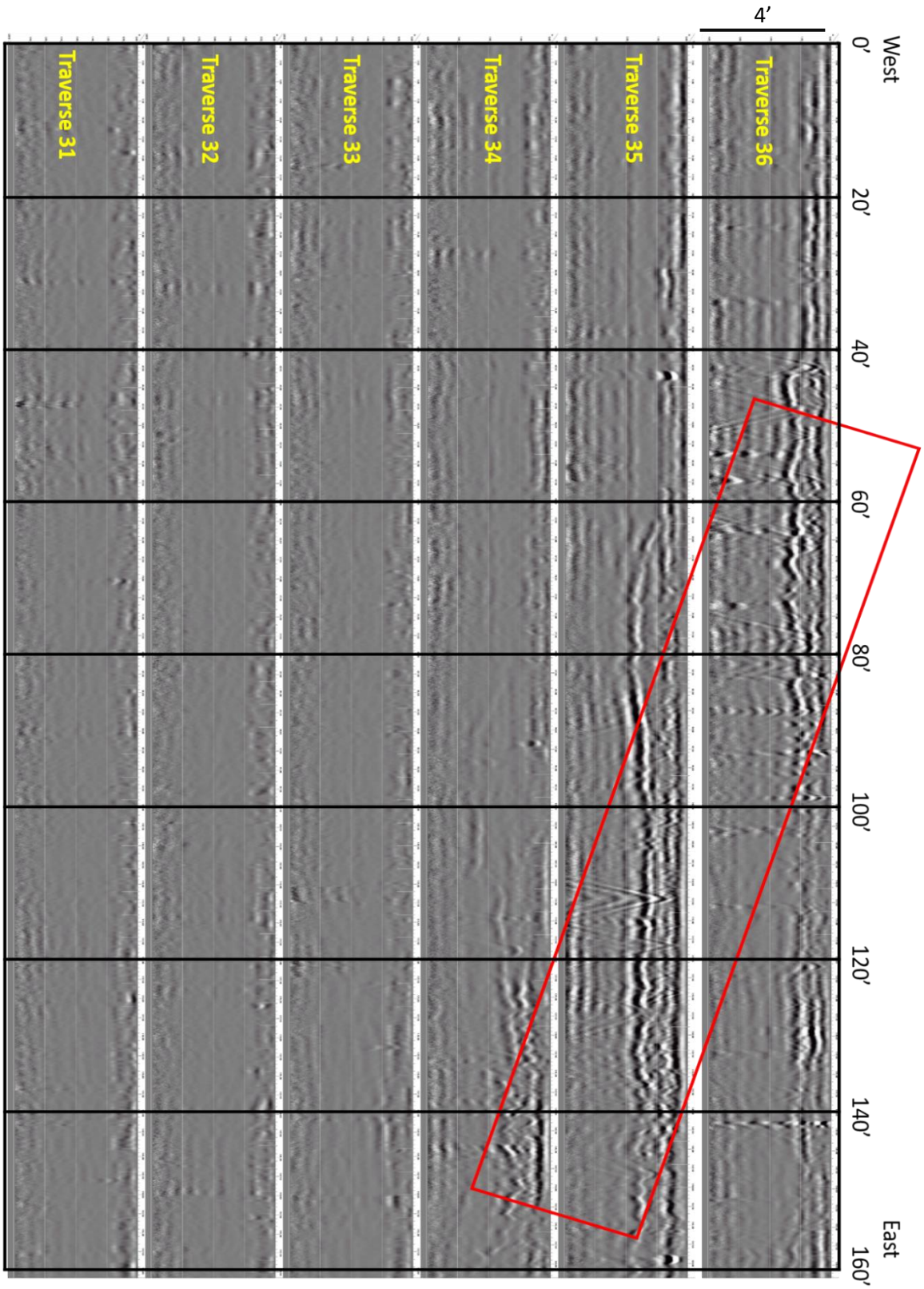

Figure A.7: GPR profiles for traverses 31-36 at Site A. Railroad spurs are visible on profiles 34-36.

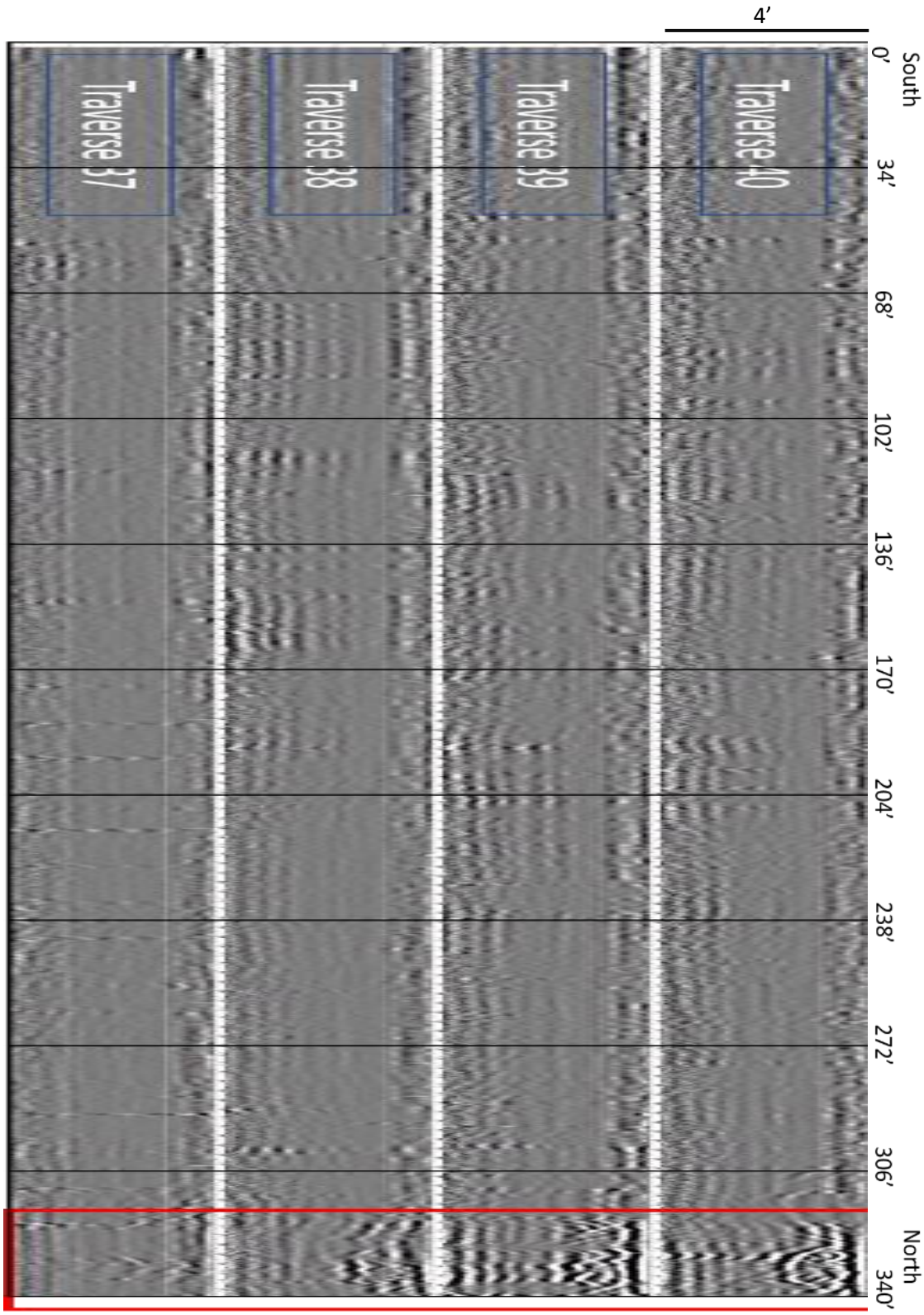

Figure A.8: GPR profiles for traverses 37-40 at Site A. Railroad spurs are visible on each profile.

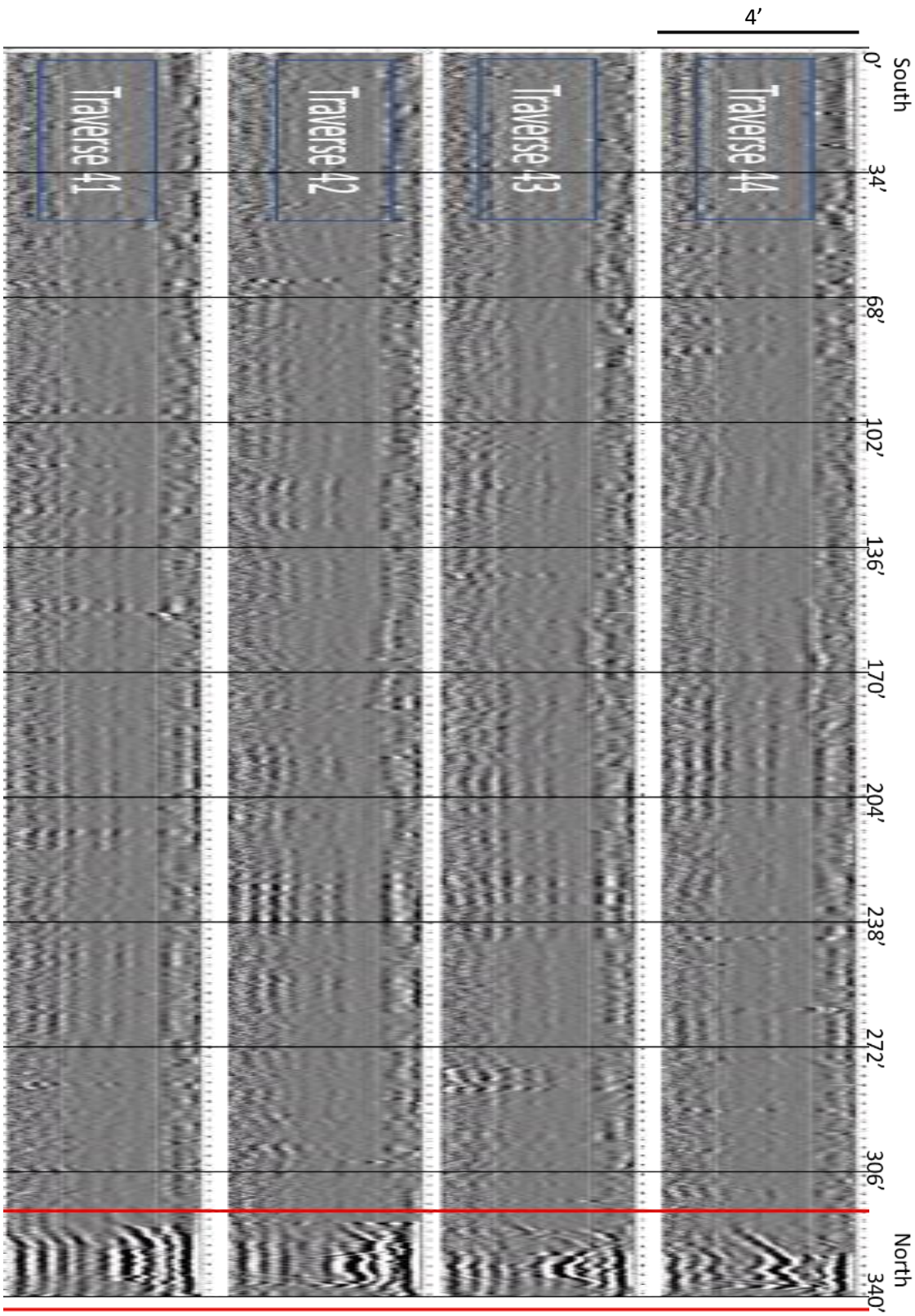

Figure A.9: GPR profiles for traverses 41-44 at Site A. Railroad spurs are visible on each profile.

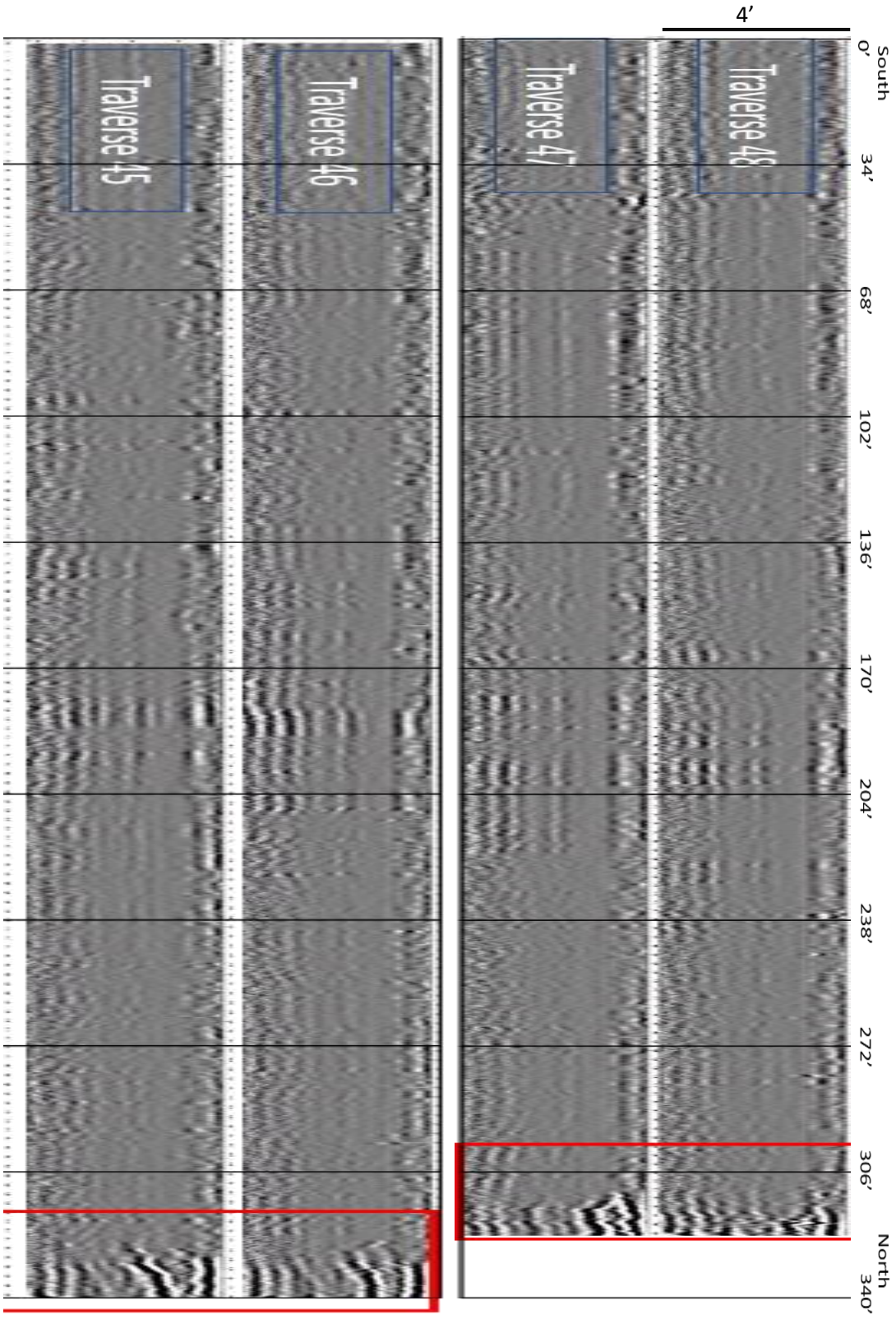

Figure A.10: GPR profiles for traverses 45-48 at Site A. Railroad spurs are visible on each profile. The offset is due to the concrete slabs.

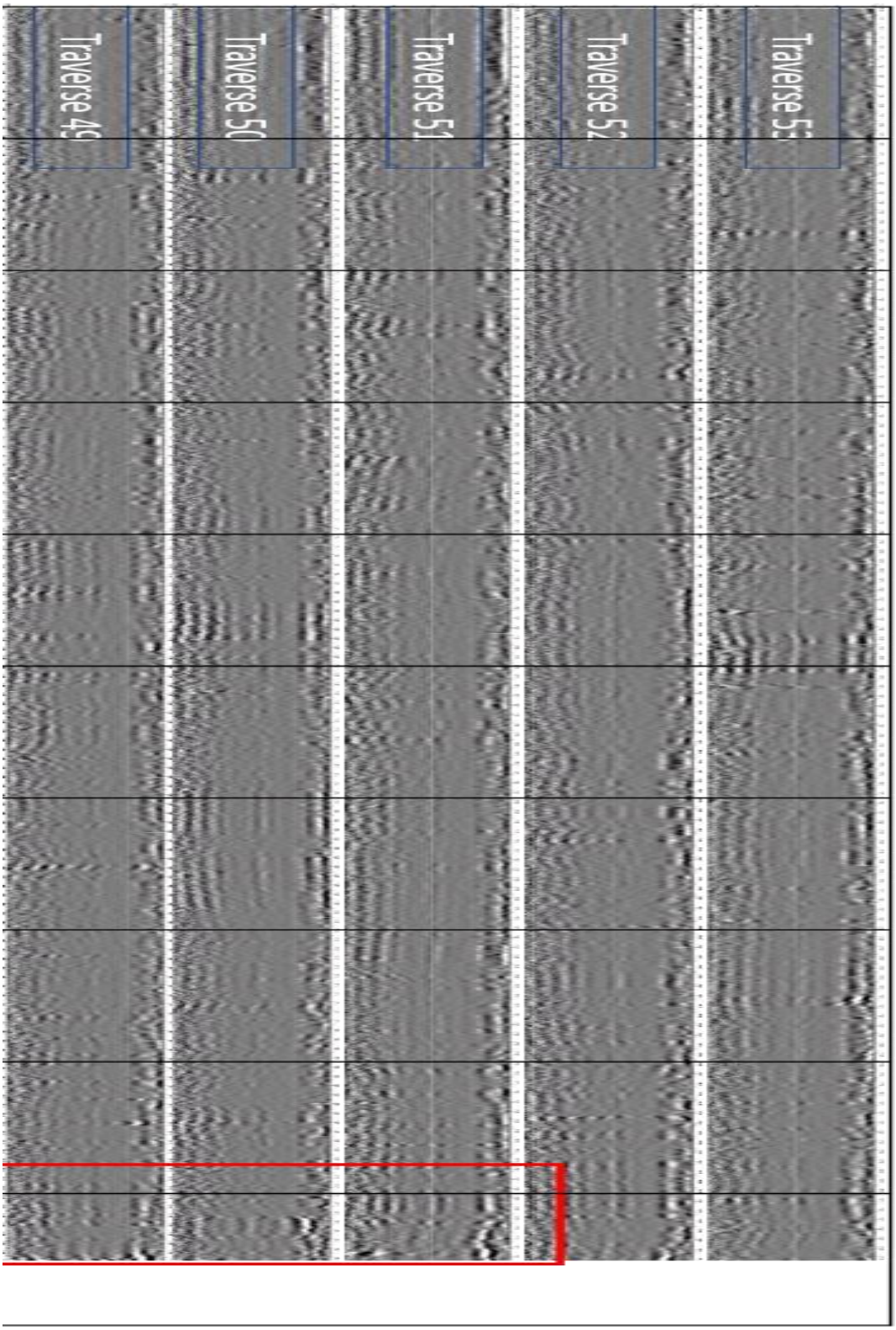

Figure A.11: GPR profiles for traverses 49-53 at Site A. Railroad spurs are visible on traverse profiles 49-51. They are not seen on profiles 52 and 53 due to the curve on the railway.

APPENDIX B.

GPR TRAVERSE PROFILES FROM SITE B AND SITE C

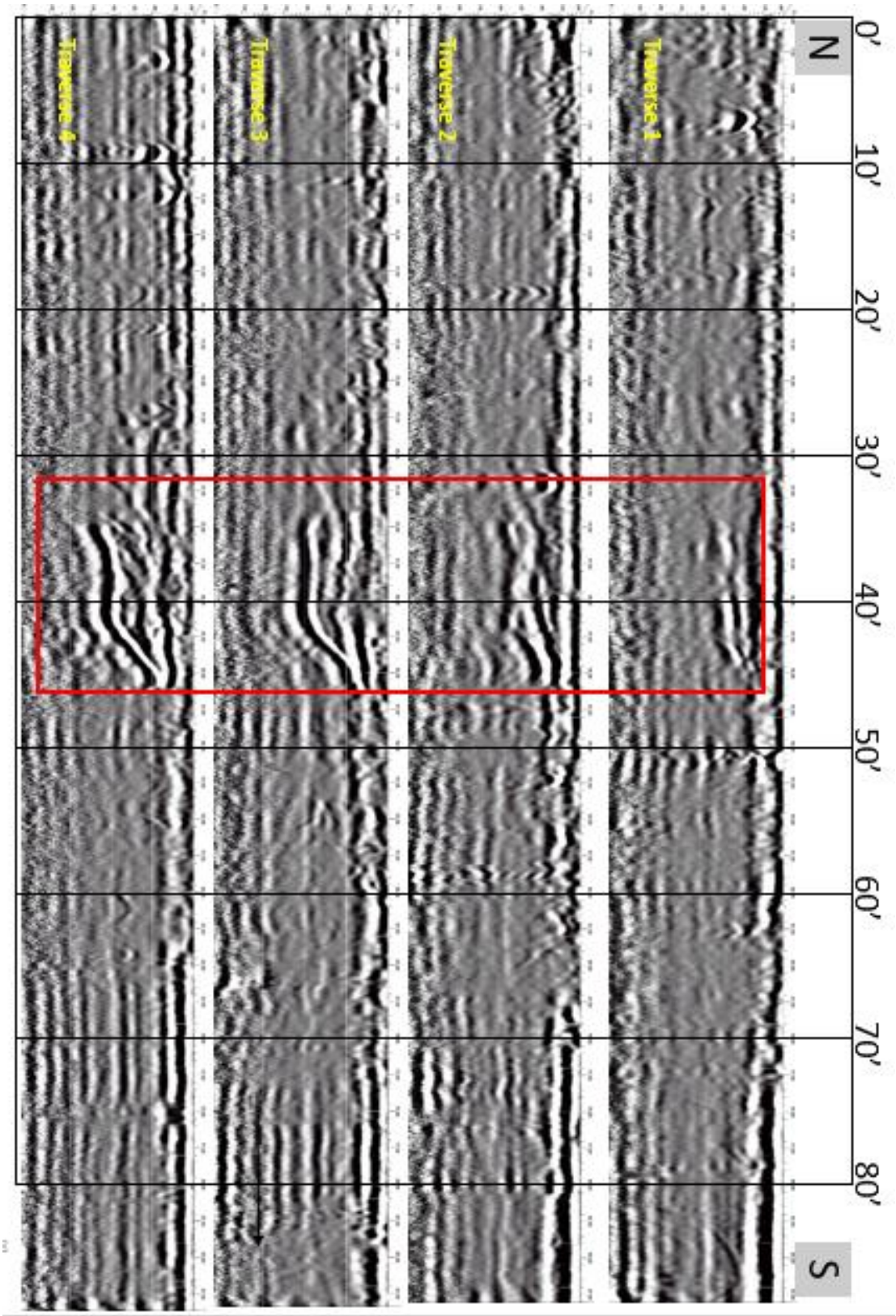

Figure B.1: GPR profiles for traverses 1-4 from Site B. Red rectangle shows potential excavation/railroad spurs.

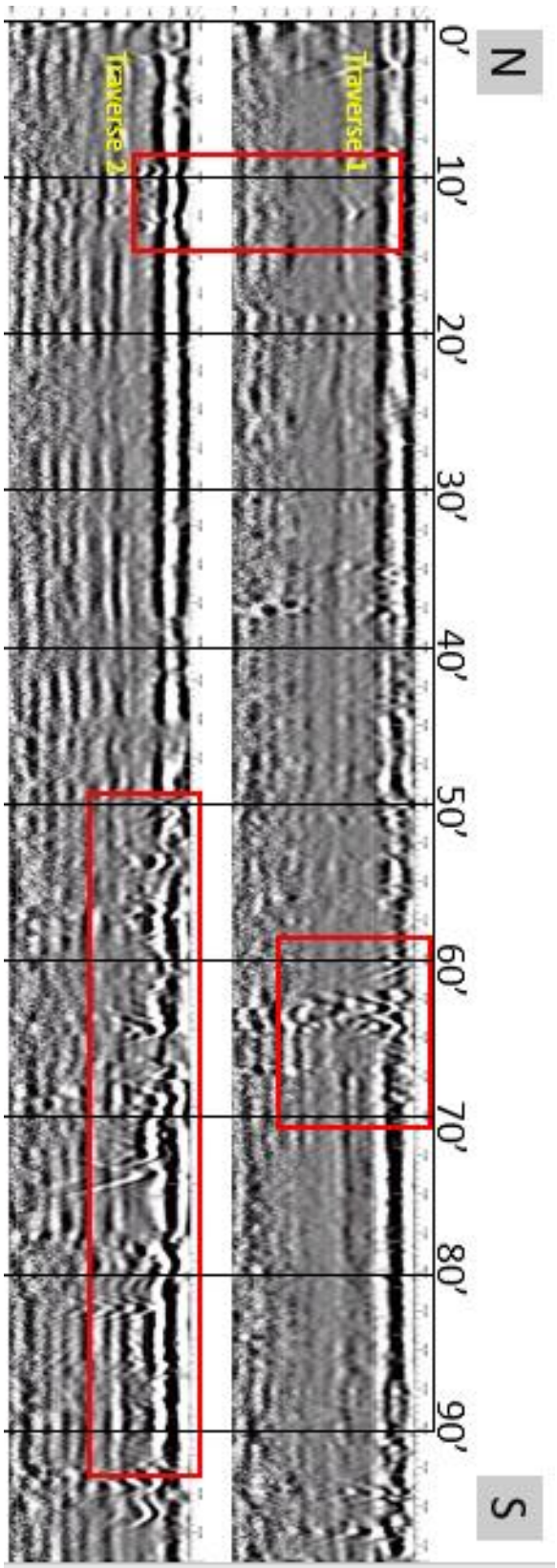

Figure B.2: GPR profiles for traverses collected at Site C. Red rectangles show anomalies caused by underground utility lines.

BIBLIOGRAPHY

Antique Ordinance, *Civil War U.S. Army Six Mule Supply Wagon.* No. 75. Antique Ordinance Publishers. Port Huron.

"Byram's Ford – Big Blue River or Westport," *Battlefields.org.* https://www.battlefields.org/learn/civil-war/battles/byrams-ford. Accessed Feb. 2019.

"Byram's Ford Road – Tour Stop #4," *Thecivilwarmuse.com, 2010,* http://www.thecivilwarmuse.com/index.php?page=byram-s-ford-byrams-ford-road.

"Guide to American Civil War in Missouri – A Brief History," *shsmo.org.* https://shsmo.org/research/guides/civilwar/abriefhistory.html. Accessed 2018.

"Price's Missouri Expedition," *Battlefields.org, 2019,* https://www.battlefields.org/learn/civil-war/prices-missouri-expedition.

Baker, G., Jordan, T., and Talley, J. (2007). *An introduction to ground penetrating radar (GRP).* Special Paper 432. The Geological Society of America.

Daniels, D. (2004). *Ground Penetrating Radar.* 2nd ed. London: The Institute of Electrical Engineers. pp.21-90.

Daniels, Jeffrey J. (2000). *Ground Penetrating Radar Fundamentals.* Department of Geological Sciences, The Ohio State University. Prepared as an appendix to a report to the U.S.EPA Region V.

Evans, David R., and David J. Ives. (1980). *Cultural Resources Survey of Proposed Sewer Construction in Kansas City, Missouri Along the Blue River and Its Tributaries, Jackson County, Missouri.* Submitted to Black and Veatch, Consulting Engineers, the City of Kansas City, Missouri, and the U.S. Environmental Protection Agency.

Fitting, James E., C. Stephan Demeter, Ronald K. Edgerton, Jeffrey C. Kimball, and Donald J. Weir. (1997). *Cultural Resources Survey of the Blue River Channel Project, Kansas City, Missouri.* Gilbert/Commonwealth Associates, Inc., Jackson, Mississippi. Submitted to the U.S. Army Corps of Engineers, Kansas City District.

French, Rowland B. (2002). *A Discussion of Geophysical Techniques: Time Domain Electromagnetic Exploration.* Northwest Geophysical Associates, Inc.

Geophysical Survey Systems, Inc. (2007). *Radan 6.5 User's Manual.* Geophysical Survey Systems, Inc. Salem.

Geophysical Survey Systems, Inc. (2009). *SIR System-3000 Manual.* Geophysical Survey Systems, Inc. Salem.

Historical Road Construction GPR Survey. *Sensoft.ca*. https://www.sensoft.ca/case-studies/historic-road-construction-2/#https://www.sensoft.ca/wp-content/uploads/2017/03/Forensics-Archaeology_pulse_EKKO-PRO-Historic-Road-Construction.pdf. Sensors & Software. Accessed 2019.

Kansas City Group. *Mrdata.usgs.gov.* 2003, https://mrdata.usgs.gov/geology/state/sgmc-unit.php?unit=MOPAkc;0. United States Geological Survey. Accessed 2018.

Marmor, J. (1997). *Prelude to Westport: Phase 1 Archaeological Survey of a Portion of the Big Blue Battlefield in Kansas City, Jackson County, MO & Addendum Archaeological Data Recovery Investigations of a Portion of the Big Blue Battlefield in Kansas City, Jackson County, MO*. TRC Mariah Associates Inc., Laramie, Wyoming. Submitted to Burns and McDonnel and the U.S. Army Corps of Engineers, Kansas City District.

McNeill, J.D., M. Bosnar (2000). *Application of TDEM Techniques to Metal Detection and Discrimination: A Case History with the New Geonics EM-63 Fully Time-Domain Metal Detector.* Technical Note TN-32, Geonics Limited, Ontario Canada.

Miller, Orloff, and Rita Walsh. (1995). *Preservation Plan and Archaeological Surface Reconnaissance for Big Blue (Byram's Ford) Battlefield, Jackson County, Missouri.* Gray & Pape, Inc., Cincinnati, Ohio. Submitted to the Historic Preservation Management Division City Planning and Development Department, Kansas City, Missouri and The Monnett Battle of Westport Fund, Kansas City, Missouri.

Nps.gov. (1993) *Civil War Sites Advisory Commission Report on the Nation's Civil War Battlefields, Technical Volume II: Battle Summaries.* [online] Available at: https://www.nps.gov/abpp/battles/tvii.htm. Accessed Feb. 2019.

Pulse 8x Hand-Held Underwater Metal Detector Operation Manual. JW Fishers MFG Inc. E. Taunton, MA.

Smith, Daniel. (2005). *Interpretive and Development Plan for Byram's Ford Big Blue Battlefield*. Monnett Battle of Westport Fund, Inc., Overland Park, Kansas. Submitted to The Civil War Round Table of Kansas City.

Web Soil Survey. *Websoilsurvey.nrcs.usda.gov*. 2018, https://websoilsurvey.nrcs.usda.gov/app/WebSoilSurvey.aspx. United States Department of Agriculture, Natural Resources Conservation Service. Accessed 2018.

Wilmarth, Mary G. (1938). *Lexicon of Geologic Names of the United States (including Alaska)*. Bulletin 896. Washington D.C.: U.S. Government Printing Office, pp. 174-175.

Yelton, Jeffrey K. (1993). *An Intensive Cultural Resources Survey of the Proposed 63rd Street Bridge Relocation at the Big Blue River, Jackson County, Missouri.* Center for Archaeological Research, Southwest Missouri State University, Springfield. Submitted to the City of Kansas City, Missouri.

VITA

Marshall Seth Foster was born on April 21, 1995, in Bethany, Missouri, a small town in northwest Missouri. He moved to Rolla to attend Missouri University of Science and Technology (Missouri S&T) after graduating high school in 2013. In May of 2017, he received his B.S. degree in Geology/Geophysics from Missouri S&T. He received his M.S degree. in Geological Engineering from Missouri S&T in May 2019.

While being a full-time student at Missouri S&T, he held multiple jobs. He worked as a Server/Bartender for four years beginning in 2015. He also was provided with a GTA position in fall of 2018, a job he was very thankful to obtain.